Brittle Fault Zones in the Mórágy Granite (South Transdanubia): New Structural and K–Ar Data

GYULA MAROS[1], BALÁZS KOROKNAI[1], KLÁRA PALOTÁS[1], BALÁZS MUSITZ[1], JUDIT FÜRI[1], JÁNOS BORSODY[1], PÉTER KOVÁCS-PÁLFY[1], PÉTER KÓNYA[1], ISTVÁN VICZIÁN[1], KADOSA BALOGH[2], ZOLTÁN PÉCSKAY[2]

[1] Geological Institute of Hungary, H-1143 Budapest Stefánia út 14.
[2] Hungarian Academy of Sciences, Atomki, Debrecen, H-4026 Debrecen, Bem tér 18/c.

Keywords: brittle deformation, gouge, granite, Hungary, illite, K–Ar, structural analysis, shear zone

Abstract

Brittle fault zones are essential elements in the structural picture of the Mórágy Granite on grounds of the results of the approximately 15-year ground-based and underground geological exploration aiming at the final deposition of low- and intermediate-level radioactive waste, which was ordered by the Paks Nuclear Power Plant Plc, and later the Public Agency for Radioactive Waste Management (Puram). They are generally steep (60–90ş), their main strikes are NE–SW, E–W, (N)NW–(S)SE and more rarely N–S. The most significant (thicker than 5 m, clay-gouge-bearing fault zone[s]), mostly NE–SW and approximately E–W striking fault zones appear about 500 m from one another according to the most reliable data source, the tunnel mapping, while the distance of the less important zones from one another is about 50-100 m. The anisotropy surfaces (rock boundaries, ductile and transitional brittle-ductile shear zones) that had formerly developed in the granite body acted as structural preformation during the formation of the fault zones in numerous cases. The evolution of the zones was basically determined by the fluids that got in and flew in the granite body after the initial cataclasis of the rock and contributed to the further weakening of the rock and also to the cementation of the zones.

Both the steepness of the zones and most of the slickenlines indicate strike-slip, oblique strike-slip movement, but at the same time, in the majority of cases no obvious kinematics can be assigned to the above mentioned strikes. Several slickenlines can often be measured in a particular zone on individual fault surfaces parallel to the zone which indicate the multiple renewals of the fault zones. Generally displacements of a few decimeters to meters can be documented along the zones.

The pattern and dip distribution of the fault zones can be basically described with the help of two brittle deformation phases, which have formed the structures of significant importance. In the kinematic model proposed an old (Mesozoic) dextral system appears first along the ?NE–SW (so-called longitudinal, approximately parallel to the Mecsekalja Zone) fault zones as major shear zones after the Variscan ductile deformations. This is followed by a Neogene transpressional dextral system along ?(N)NW–(S)SE striking transversal planes as major shear zones. Presumably, a sinistral longitudinal system also evolved between the two phases and another one after them; these were active during the intrusion of the Cretaceous alkaline basalt dykes and the elevation of the Mecsek Mts. and the Mórágy Block, respectively.

K–Ar age determinations from the most intensively deformed clay fault gouges of the fault zones were carried out. The polytype of illite is predominantly 1M that refers to hydrothermal genetics. The age determinations obtained on illite-rich fine fractions provided rather scattered Mesozoic (Middle/Late Triassic – Late Cretaceous) ages, indicating multi-phase illite formation in the research area. The oldest (Triassic) ages can be qualified as most reliable on grounds of different mineralogical/structural considerations (mixed illite/smectite structure and quantity of smectite, FWHM values, presence of other “disturbing” phases), so they probably indicate the age of real brittle structural event(s), which seem to be supported by the widespread regional occurrences of such ages. Although with a bit greater uncertainty, the same of the Late Cretaceous ages can be supposed. The geological meaning of the Middle Jurassic and the Early Cretaceous ages is problematic owing to the uncertainty of the genetic connection between the considerable amount of illite/smectite or smectite in these samples, and the dated 1M illite.

Introduction

Brittle fault zones, formed by rigid deformation in relatively small, sheet-like rock volumes of the upper crust (<10 km), represent the most complex structural objects of brittle deformation. In this work the brittle fault zones of the Mórágy Granite exposed in the northeastern part of the Mórágy crystalline block are discussed. The structural investigations—as an integral part of the geological research on the final disposal of nuclear waste of low- to intermediate activity—were carried out in various research objects as boreholes drilled during the ground-based and underground geological research phases (MAROS et al. 1999; DUDKO 2000; MAROS, PALOTÁS 2000a–b; ZILAHI-SEBESS et al. 2000; MAROS et al. 2003, 2004; SZONGOTH et al. 2003; BALLA et al. 2003, 2008; BALLA 2004; ZILAHI-SEBESS 2005; MAROS 2006; and references therein), surface outcrops (DUDKO, SZEBÉNYI 2003; MAROS et al. 2003; GYALOG et al. 2006), exploratory trenches (GYALOG et al. 2003), furthermore inclines (MOLNOS et al. 2006, 2007, 2008). The research was ordered and financed by Puram.

Detailed investigation of fault zones transsecting the granite body is of basic importance in order to characterise properly the geological medium of the nuclear waste repository. Beside the rock mechanical aspects, fault zones play also a crucial role in the hydrogeological features of the repository and its near surroundings, since they can serve both as barriers or especially good conducting zones for fluid migration. Moreover, authors' experiences show that these features can even change along the strike of a given fault zone. In this study first the main types and geometrical characteristics of fault zones will be introduced, then an overview will be given on the microstructural and mineralogical properties of clay-gouge-bearing fault core zones, furthermore also on the spatial distribution and kinematics of fault zones, finally their age and formation mechanism will be discussed.

Up to now, structural documentation of 358 fault zones was carried out in the different research objects. Structural data of a given zone may belong to one, relatively well-defined zone with a specific strike or to a relatively smaller, separately documented zone that forms an individual branch of a larger fault zone.

The type, elaboration and reliability of the documentation is somewhat different in the different research objects, consequently there are also differences among the numbers of elements of the applied evaluation categories (e.g. orientation, thickness). There are, for instance, altogether 358 fault zones, from which 323 zones have their own orientation data, and 319 zones have their own thickness data. In the case of inclines—in order to avoid data redundancy and consequent distorting effect—only one measured orientation datum for an individual fault zone plane was always considered if its correlation was quite unambiguous between the two tunnels.

Geological Setting

The research area located in the northeastern part of the Mórágy crystalline block (JANTSKY 1953, 1979) belongs to the so-called Mecsek Zone representing the northernmost, Alpine tectonic subunit of the Tisza Unit (Figure 1). Among the pre-Cenozoic rocks of the Mórágy crystalline block granitoid rocks assigned to the Mórágy Granite Formation (BALLA et al. 2003) prevail. The NE–SW trending granite body is bounded by the similarly NE–SW trending and steeply NW-dipping Mecsekalja Zone from the NW in which mylonitic, Lower Palaeozoic metamorphic rocks are exposed. At the northwestern margin of the Mórágy Block non-metamorphic, Lower Jurassic sediments have a sharp tectonic contact with the mylonitic metamorphites. All of the previously mentioned rock series are crosscut by Cretaceous alkaline volcanic dykes of various composition ("bostonites"; MAURITZ, CSAJÁGHY 1952). These pre-Cenozoic basement rocks are discordantly overlain by Neogene or Quaternary sediments.

The Lower Carboniferous (≈340 Ma: KLÖTZLI et al. 2004; GERDES 2006) Mórágy Granite is composed of two major lithological elements: microcline megacryst-bearing biotite monzogranites and mafic enclaves of predominantly monzonitic composition. These rocks were formed by the mixing and mingling of two different magmas in the early phase of the magmatic evolution (BUDA 1999; BUDA et al. 2000; KIRÁLY, KOROKNAI 2004; BUDA, DOBOSI 2004), defining also the magmatic structure of the pluton (MAROS 2006). Structural phenomena observed in the Mórágy Granite can be related to three main deformation regimes (magmatic, ductile and brittle). The different deformations can be attributed to two major orogenic cycles (KOROKNAI 2009; MAROS, KOROKNAI, 2009):

1) The predominant NE–SW trending structure of the granite body was achieved during the ***Variscan*** orogenesis. The Variscan tectonics can be divided into two major stages:

1a) Both the early and late phases of the *magmatic stage* are characterised by the formation of NE–SW trending structures (rock boundaries, contamination planes, elongate-flattened mafic enclaves, and leucocratic dykes). The well-defined orientation of these phenomena suggests the presence of an active, non-hydrostatic stress field during the magmatic evolution.

1b) Ductile deformation associated with the *metamorphic stage* of the Variscan tectonics produced two, also NE–SW trending, rather steeply dipping foliation generations, furthermore mylonitic zones and folds in the already solidified pluton. Beside these ductile structural elements, the formation of coeval brittle faults—as well as in the magmatic stage—is also supposed, although this assumption is difficult to prove directly.

2) The second main tectonic event is represented by the ***Alpine*** orogenesis in the course of which numerous brittle deformation phases occurred, including here also the intrusion of Cretaceous alkaline volcanic dykes into the pluton. Brittle fault zones discussed in this study are the products of the ***Alpine***

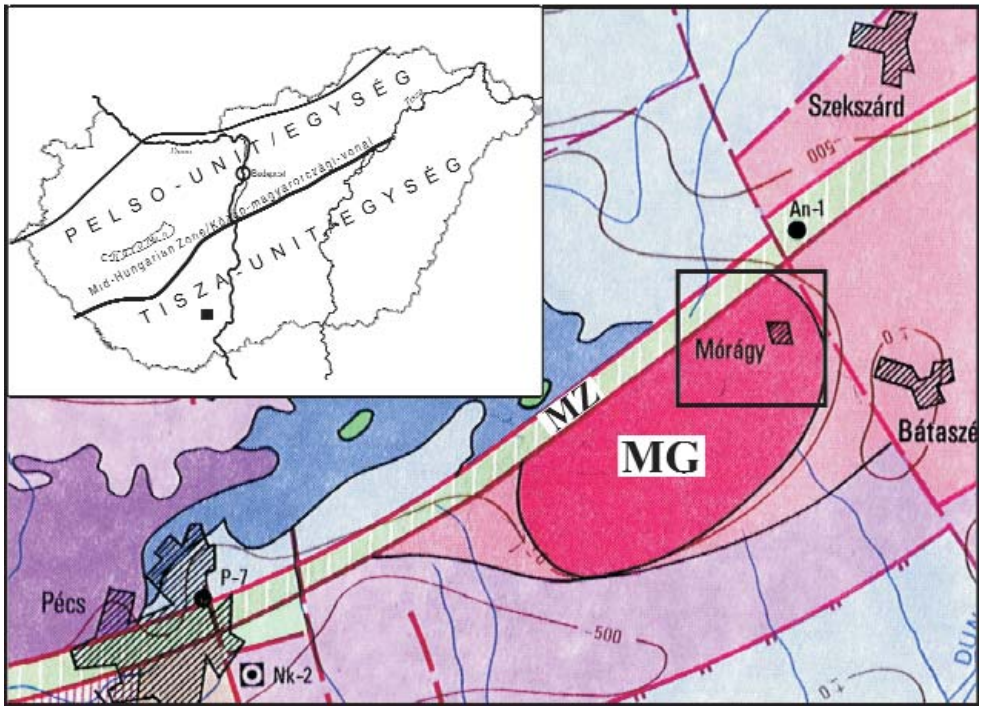

Figure 1. Pre-Cenozoic geological overview map of the Eastern Mecsek Mts. and the Mórágy crystalline block (after FÜLÖP 1994)

The study area is indicated by the black rectangle; red = Mórágy Granite, purple = Triassic, blue = Jurassic, green = Cretaceous rock series (the lighter tones indicate the subsurface distribution of the individual rock series); MZ = Lower Palaeozoic metamorphic rocks of the Mecsekalja zone, MG = surface distribution of the Mórágy Granite; top left: generalised tectonic map with the study area (black square)

1. ábra. A Keleti-Mecsek és a Mórágyi-rög áttekintő prekainozoos földtani térképe (FÜLÖP 1994 nyomán)

A vizsgált terület helyzetét a téglaalap jelzi; piros = Mórágyi Gránit, lila = triász, kék = jura, zöld = kréta képződmények (a világosabb színárnyalatok az egyes képződmények felszín alatti elterjedését mutatják); MZ = Mecsekalja-zóna ópaleozoos metamorf képződményei, MG = a Mórágyi Gránit felszíni elterjedése; bal felső sarokban: vázlatos nagyszerkezeti térkép a kutatási terület (fekete négyzet) feltüntetésével

tectonics mainly; however, some of them may represent pre-existing, reactivated Variscan fault zones.

Structure and Types of Fault Zones

Fault zones are generally about tabular or sheet-like zones with planar or undulating surfaces, where rocks are much more intensively deformed than in their environment. Their typical thickness ranges between a few cm – a few 10s m in the research area.

Several basic types can be distinctly distinguished among the documented fault zones on the grounds of the characteristic structure of their most intensively deformed zone (Figure 2). The basic types that have been identified in the research area can be arranged into an evolutionary succession (MAROS 2006) on the basis of the increasing intensity of the deformation (Figure 2). Various types can occur—even repeatedly—within one fault zone, in this case the classification of the fault zone happens by the type showing the most intensive deformation. An important factor is when a zone is developing that the degree of deformation generally varies in different rock variations of the granitoid body, and not rarely, the orientation of a zone (e.g. foliation, transitional brittle-ductile shear zones [so-called "pseudo-mylonites"]) largely preform a fault zone during its development.

The "least developed" fault zone is *fault bundle* which is a dense set of faults running approximately parallel to one another (Figure 2, 1). The number of faults is 5–10 or more, the distance between faults is generally 2–20 cm. *Braided-sigmoidal* strike-slip or inverse *duplexes* evolve with the intensity of deformation increasing (BOYER, ELLIOTT 1982, RAMSAY, HUBER 1987). In this case the brittle deformation advances not only along one plane but about parallel planes that are connected with "deformation bridges". The geometry of the latter follows the direction of the so-called P faults, which commonly do not crosscut the major faults but bend into them. This finally leads to the formation of sigmoidal structures, which were called "deformation fish" after their characteristic shape during the documentation. The originally neighbouring rock bodies partly "creep" upon one another (or near one another in the case of strike slips) along the boundaries of fish, such multiplying the original thickness (Figure 2, 2). The intensively deformed, rather narrow core zone cannot be distinguished clearly within the comparatively thick braided-sigmoidal or bundled fault zones to authors' experience.

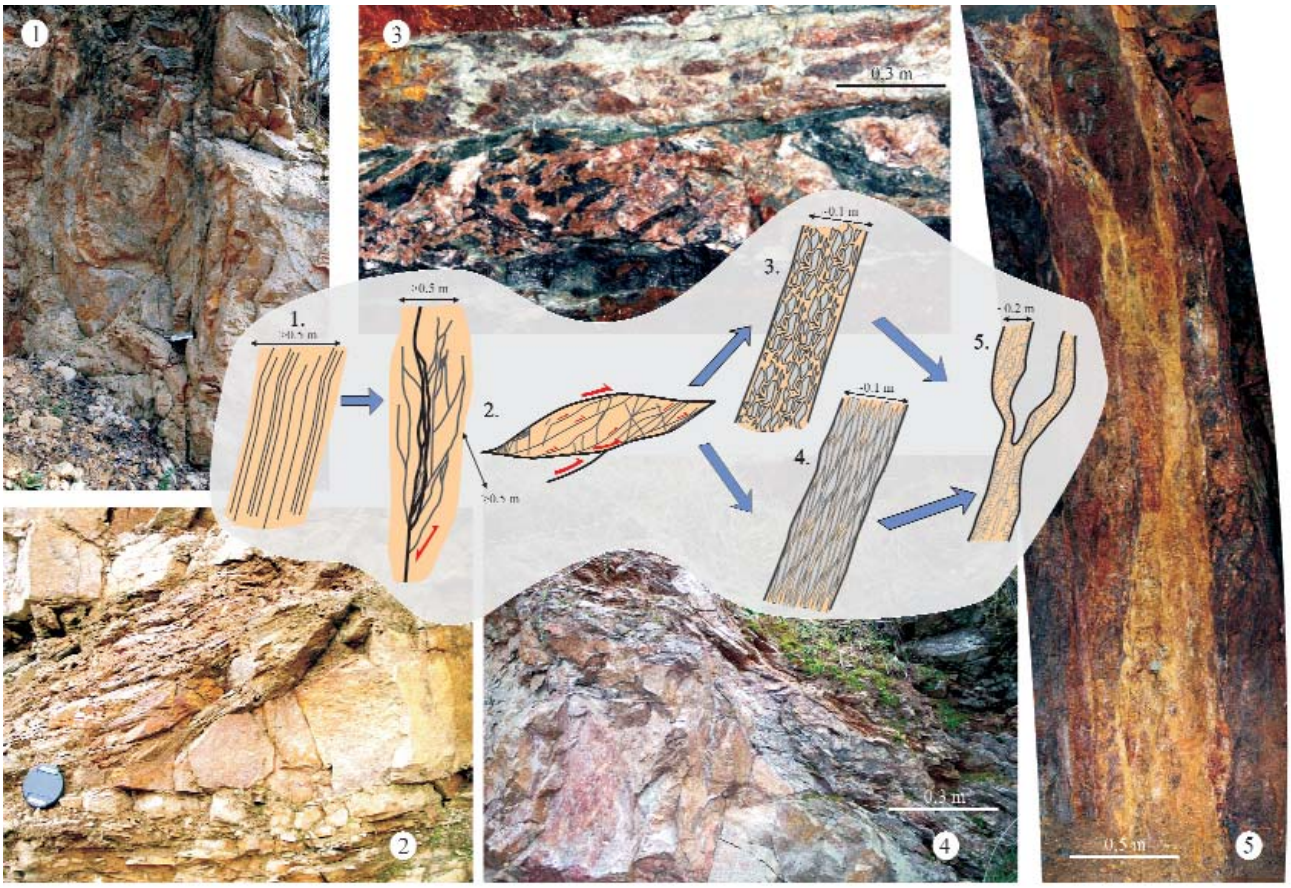

Figure 2. Basic types of fault zones on grounds of the structure of their most intensively deformed zone

The arrows indicate the possible transitions between the different types as the intensity of the deformation increases; 1—fault bundle, 2—braided-sigmoidal strike-slip or inverse duplex, 3—flaky, 4—brecciated, 5—rubbled with clay fault gouge

2. ábra. A törészónák főbb típusai a legintenzívebb deformációt elszenvedett zónájuk felépítése alapján

A nyilak a különböző típusok közötti lehetséges átmenetek irányát mutatják a deformáció intenzitásának növekedésével; 1 – törésnyaláb, 2 – fonatos-szigmoidos eltolódásos vagy feltolódásos duplex, 3 – leveles, 4 – breccsás, 5 – murvás, vetőagyagos

Now the evolutionary succession divides into two: *(a) Brecciated* structure develops by the break-up of the sigmoids (BILLI et al. 2003; Figure 2, 3). Clay gouge often occurs in the fine-grained matrix of the breccia besides other infilling materials, the breccia pieces and grains are constituted recognisably mostly by the debris of the sigmoids. *(b)* The other possibility is *flaky fault zone* (Figure 2, 4), which is constituted by several mm-thick rock sheets and very thin argillic stripes in between. The rock flakes can be considered in most cases as very intensely flattened sigmoids that can develop by splitting the sigmoids of the braided-sigmoidal type into pieces. The foliated or mylonitic structure that had developed during the previous deformation of the rock, as well as the petrological composition essentially influences the formation of the flaky type. So flaky fault zones typically develop in fine-grained, biotite-rich monzonitic, as well as intensely foliated rocks, while brecciated structure evolves mainly in non- or slightly ductilely deformed, relatively coarse-grained rock types. In this sense the "heritage" of a mylonitic structure into brittle deformation can be observed in a lot of places.

With further increasing the intensity of the deformation, the "flakes" do not split into thinner parts in the case of the flaky structure but break up first perpendicularly to their long axis then parallel to it (BILLI et al. 2003). The breccia pieces also break up further into smaller fragments in the case of brecciated structures. As the process advances, the meanwhile isometric grains start rotating, the rock is deformed by so-called cataclastic "flow" (ENGELDER 1974). This is how the *rubbled* type with *clay gouge* (Figure 2, 5) evolves to be the "most developed" type of all. The rock fragments either crumble into clay fraction during the deformation or become rounded, maybe sharp-edged grains. At places the fragments of different fractions are arranged along planes parallel to the displacement (so-called C plane) or along planes closing an acute angle with it, this is how a rock structure similar to S–C foliation (PASSCHIER, THROUW 1996), known from the ductile regime, can develop in these rocks. This is called foliated clay fault gouge. The argillation of the crumbled fault gouge—as well as the usually multi-phase, often tectonically (even multiply) reworked, different hydrothermal infillings (mostly carbonates and Fe-oxides, -oxihydroxides and -hydroxides) that are almost always present in fault zones—indicate the important role of fluids moving in the zone during the deformation. This type can even repeatedly occur in the inner, most intensively deformed part of a significant fault zone.

The individually documented, narrower zones unite in lenticular, sigmoidal fault zone bundles in a lot of cases (Figure 3). So fairly intact, isolated rock bodies, very fractured rocks and—concentrating most of the deformation—fault rocks (fault breccia, cataclasite, clay fault gouge) can be found in the complex system of fault planes that join in the fault zones. The stress field has yielded in a rather heterogeneous deformation in the given rock volume.

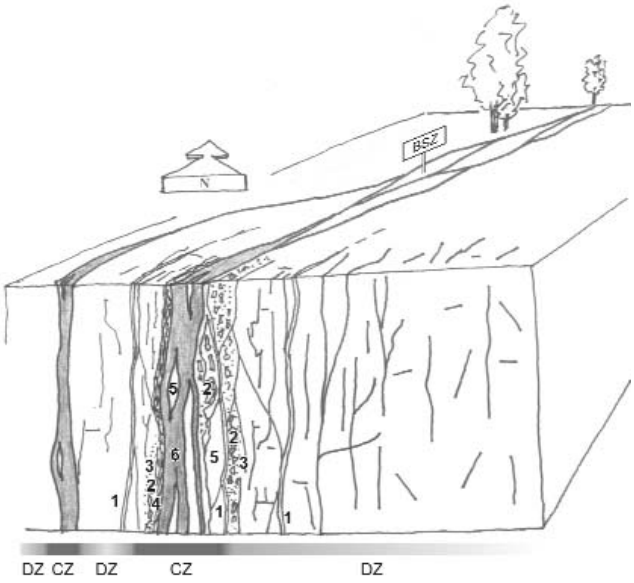

Figure 3. Theoretical model of a branch of fault zones

BSZ = branch of fault zones, CZ = core zone, DZ = damage zone; 1–infilling, 2–breccia, 3–cataclastic protolith, 4–flaky zone/"pseudomylonite", 5–intact sigmoid, 6–foliated clay fault gouge

3. ábra. Törészónaköteg elvi modellje

BSZ = törészónaköteg, CZ = magzóna, DZ = kárzóna; 1 – kitöltés, 2 – breccsa, 3 – kataklázosodott protolit, 4 – leveles zóna/„pszeudomilonit", 5 – intakt szigmoid, 6 – foliált vetőagyag.

Fault zones can be divided into a so-called damage zone and a core zone (Figure 3) depending on the degree of deformation (Chester, Logan 1986, Caine et al. 1996, Wibberley, Shimamoto 2003, Faulkner et al. 2003). The core zone—which often includes clayey fault rocks in the Mórágy Granite—can have a transitional or sharp boundary, it is called "master fault" in the latter case. The master faults situated on both sides of the core zone are parallel to the fault zone as a rule (Billi et al. 2003) and according to authors' experience they are generally distinctly observable structural elements. The resultant displacement in the fault zones equals to the total displacements along fault planes next to one another.

The appearance of the brecciated, flaky or rubbled (with fault gouge) types can be connected characteristically to fault zones with distinct core zone(s).

Thickness Relationships of Fault Zones

The thickness relations of fault zones is illustrated by Figure 4, a), according to which the average thickness of fault zones is generally (more than 90%) is a few (<5) m. The number of zones thicker than this radically decreases towards the maximum thickness (35.5 m). A decreasing trend can also be noticed among the zones of 0–5 m thickness (Figure 4, a) which constitute the bulk of the data, towards the greater thickness, although the degree of decrease is less radical than in the case of zones thicker than 5 m. The thickness distribution tends distinctly to a logarithmic graph

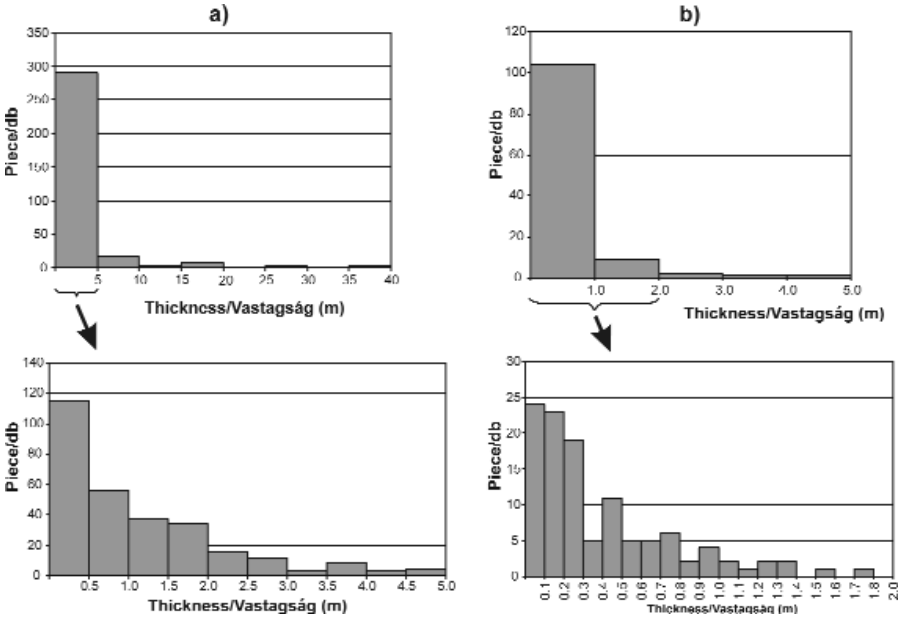

Figure 4. Thickness distributions of fault zones

a) all fault zones, b) clayey core zones

4. ábra. Törészónák vastagságeloszlásai

a) összes törészóna, b) vetőagyagos magzónák

(correlation coefficient R^2=0.9225). The thickness relations of the clayey core zones (Figure 4, b) of the "developed" fault zones that accumulate the bulk of the deformation have also been studied besides the total thickness of the zones. The thickness distribution of clayey core zones (117 altogether) shows basically the same trend as the thickness distribution of all fault zones, so the occurrence very quickly decreases towards the greater thicknesses. The thickness of the clayey core zones is smaller than 1 m (generally a few dm) in the decisive part (>90%) of the cases; only four were thicker than 2 m. The distribution of clayey core zones narrower than 2 m (almost 97% of all data) also tends distinctly to a logarithmic graph (correlation coefficient R^2=0.8748).

To describe the structural significance (order[1]) of the fault zones, a combined scale was used, which had been developed by means of experience and is based on structural criteria. One basic assumption of the classification is the thickness of a zone (>10 m—Class 1, 5–10 m—Class 2, 2–5 m—Class 3, <2 m—Class 4). The base of the other "subscale" is whether a given zone contains a distinctly distinguishable clayey–rubbled core zone that accumulates the bulk of the deformation. The fault zones that do not contain clayey core zone have been divided into two groups according to their state of development (fault bundle—Class 4, braided–sigmoidal—Class 3). The fault zones that contain clayey core zone(s) have also been divided into two groups according to the number of cores (one core zone—Class 2, more than one core zones—Class 1). The structural significance of the studied fault zones can be characterised with one single number between 1 and 4 by the combination of the two subscales (namely averaging the two values for each zone). At the same time, it seems to be important to stress that the structurally "most significant"—according to the thickness and "development" of a given zone—qualification does not necessarily coincide with the hydrogeological significance of a fault zone (e.g. Péter Fault) which is not particularly important from structural geological point of view—it merely received 2.5 points in the above scale—, plays an outstanding role in the hydrogeological system of the area).

The distribution of fault zones according to their structural significance (Figure 5) is very similar to that of the thickness distributions: the number of occurrences decreases very rapidly towards fault zones of greater importance. The number of the most significant (Order 1–2) fault zones that are thicker than 5 m and contain a clayey core zone is small, their proportion scarcely exceeds 10%. In the followings they are called first-order fault zones. The bulk of the data (88%) is constituted by zones that are less than 5 m thick and usually do not contain clayey core zone. This group can be further divided into two parts: the thickness of the second-order (significance between 2.5 and 3) zones exceeds 2 m and they often contain clayey core zones. The thickness of the least important (significance between 3.5 and 4) fault zones that lack clayey core zone is less than 2 m. There is a difference if the distributions of structural significance and thickness are compared, namely that the quantity of the least important (Order 4) zones is smaller than that of zones Order 3 and 3.5 (the number of the narrowest zones is always the largest at the thickness distributions). The reason probably is that the classification/distinction of narrow (<2 dm) fault zones during field documentation is rather subjective. Part of these zones has been described as individual fault with thick infilling, and, on the other hand, the recognition and classification as fault zones of certain types (e.g. fault bundle) is not unambiguous in all cases. The dip distribution of the different groups is discussed in Chapter "Dip Distribution of the Fault Zones".

[1] By order size, significance now and later on are meant

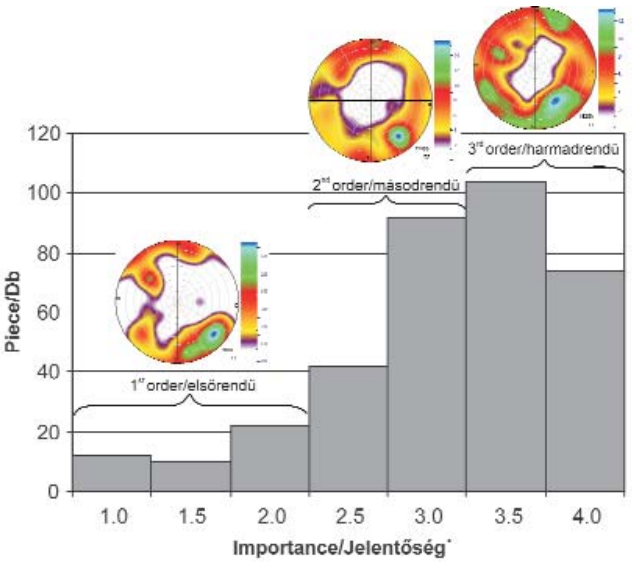

Figure 5. The distribution of fault zones of different orders based on the scale that considers the whole thickness and the "development" of the zones

The stereograms show the orientation of fault zones of different orders. See details about the scale in the text. The stereograms are in lower hemisphere projection. In the bottom right corner of the stereograms the number of data, in brackets the number of slickenlines is displayed

5. ábra. A különböző rendű törészónák eloszlása a zónák teljes vastagságát és „fejlettségét" figyelembevevő skála alapján

A sztereogramok a különböző rendű törészónák térbeli irányítottságát mutatják. A skála részletezését l. a szövegben, a sztereogramok alsófélgömb-vetületben készültek. A sztereogrammok jobb alsó sarkában az ábrázolt adatok száma, zárójelben az ábrázolt vetőkarcok száma látható

Internal Structure of Clay-gouge-bearing Fault Core Zones

In the followings—using a progressively focusing approach on selected examples—the macro- and microscale results on the internal structure and build-up of the studied fault zones will be introduced. Furthermore, an overview is also given on their most important mineralogical properties. Investigations were carried out on samples deriving from the "most evolved", clay-gouge-bearing fault zones exposed in the tunnels, since these zones and their surroundings were mapped with a special care, furthermore this type of fault zones bears the most valuable information on the whole deformation process.

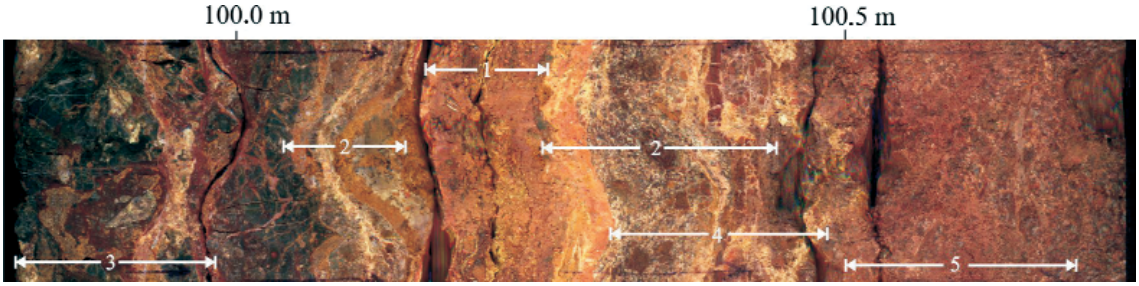

Figure 6. Detail of a clay-gouge-bearing fault zone from the Pilot Borehole BeK–1 (99,75–100,75 m)
1—clay gouge, 2—zones crosscut and/or infiltrated by hydrothermal infillings, 3—breccia, 4—"hardened", cemented clay gouge, 5—cataclasite, breccia

6. ábra. Murvás, vetőagyagos törészóna részlete (99,75–100,75 m) a BeK–1 jelű vágatelőfúrásból
1 – vetőagyagos magzóna, 2 – kitöltések által átjárt és cementált zónák, 3 – breccsa, 4 – „felkeményedett" magzóna, 5 – kataklázit, breccsa

The internal structure of these fault zones can be studied excellently in the near-horizontal pilot boreholes displaying a particularly good core recovery (Figure 6). Characteristic features of fault zones of different type introduced above appear—as it is obvious from the photo—in the discussed clay-gouge-bearing fault zone as well. The damage zone showing variable intensity of fracturing, but generally only a minor degree of mineralogical alteration is bounded first by a breccia zone, which is followed by a several decimetre thick zone cut by a larger number of veins. Next to this zone a (or in other cases: several) clay-gouge-bearing zone is exposed that accommodates the most of the deformation in the core of the fault zone. If the fault zone contains more than one clay-gouge-zone, they are generally accompanied with veins, breccias, cataclasites, or any combination of these fault rocks between the individual gouge zones. The rheological properties of the most intensively deformed clay gouges, however, may change substantially during (or after) the deformation ("strain hardening") due to hydrothermal "cementation". In this case the deformation—during progressive deformation—may "jump" into a new clay-gouge zone, or it can rework the previously "hardened", infilling-rich clay-gouge zone producing mostly breccias during this process. In the drillcores and tunnels many times fault zones with several clay-gouge zones were observed, furthermore (even many times) reworked vein infillings occur also in the fault zones exposed in the outcrops. Therefore, the change of active deformation zones within an individual fault zone, furthermore the reactivation of certain faults can be regarded as a relatively frequent phenomenon in the research area.

In the followings the internal structure of the most intensively deformed clay gouges will be characterised based on microscale observations. In order to illustrate their most indicative features, a nearly vertical, E–W striking, strike-slip fault zone (so-called "Peter Fault") was selected from the investigated, 15 most important fault zones (altogether 33 samples). This zone, acting hydrogeologically as a major barrier, was carefully mapped in the Eastern Incline in the section 1392.9–1393.9 m and in the section 1450.6–1452.1 m of the Western Incline, respectively.

In the sample studied the fine-grained, brownish, clayey matrix often contains anisometric (elongate), occasionally sigmoid-shaped, cm-sized granitoid clasts (Figure 7), furthermore reworked clasts deriving form earlier carbonate vein infillings. The microstructure of this rock is strongly oriented that is also well-reflected in the arrangement of the often elongate granitoid clasts that show a preferred orientation according to their long axis. This fault rock formed in the brittle regime displays—as well as ductile mylonites—several foliations: one of the foliations (C planes; ca. horizontal on the photo) is parallel to the main shear planes. There is an other, also well-visible, sigmoid-shaped foliation (P) merging into the main (C) shear planes on the left side of the photo. The pattern defined by these two foliation systems is perfectly analogous with the S–C foliation formed in the ductile regime, and indicates a dextral sense of shear on the photo that corresponds to strike-slip motion regarding the original geographical orientation of the sample. The geometry of shear bands (so-called C' planes corresponding practically to brittle, synthetic Riedel shear planes) in the upper and right side of the sample indicates dextral sense of shear, too. The high proportion

Figure 7. Cut surface of a foliated clay fault gouge deriving from the core zone of the Péter Fault penetrated between 1392.9–1393.9 m in the Eastern Incline
The S–C geometry of the foliation planes (left side) and the shear bands (upper part and right side) indicate dextral sense of shear in the present position. The original position of the cut surface is horizontal

7. ábra. Foliált vetőagyag elvágott felülete a Keleti lejtősakna 1392,9–1393,9 m között harántolt törészóna magzónájából
A foliációs síkok S-C geometriája (bal oldalon) és a nyírószalagok (felül és jobb oldalon) jobbos nyírást jeleznek a képnek megfelelő helyzetben. A minta vágott felületének eredeti helyzete vízszintes

(40–50 wt%) of the fine-grained matrix containing mainly clay minerals (illite, smectite, palygorskite) and chlorite suggest intense fluid flow in the fault zone. Foliated (micro)structure was also observed in an other sample of the same fault zone collected in the Western Incline (1450.6 m). This fact indicates that the clay-gouge-bearing core zone of this E–W striking fault can be directly correlated between the two inclines.

A thin (several mm thick) clay-gouge sample (Figure 8, a) deriving from an other locality of the same fault zone can be well studied also at microscopic scale. This clay gouge containing angular, mostly isometric rock and mineral fragments does not exhibit a foliated structure. These features—both separately and together—clearly suggest a less intense deformation in this sample than it was in the previously described, foliated clay gouge. The clay gouge has a very sharp contact crosscutting the adjoining, also thin, transitional brittle-ductile shear zone ("pseudomylonite") with oriented microstructure and frequent sigmoid-shaped rock and infilling fragments, that represents the product of an earlier deformation phase (MAROS 2006; MAROS, KOROKNAI 2009). The "pseudomylonite" may have acted as a pre-existing weakness zone affecting the deformation of the rock during the formation of the brittle fault zone. Both fault rocks have sharp contacts with the protolith crosscut by a network of fractures filled mainly by clay minerals.

The boundary between the cataclased protolith and the clay gouge is, however, not always sharp, but a more or less gradual transition can be observed in other cases (Figure 8, b). The transitional zone is characterised by fault rocks that differ in their microstructural properties (size and quantity of clasts, presence/absence of foliation). A given fault rock stripe with characteristic microstructure may appear even several times. The alternation/repetition of fault rocks with somewhat different microstructure seems to be very similar to the internal structural features of fault zones observed on larger (outcrop) scale. The sample is crosscut—both parallel and different angle to the strike of the fault zone—by different generations of fractures filled mainly by carbonates.

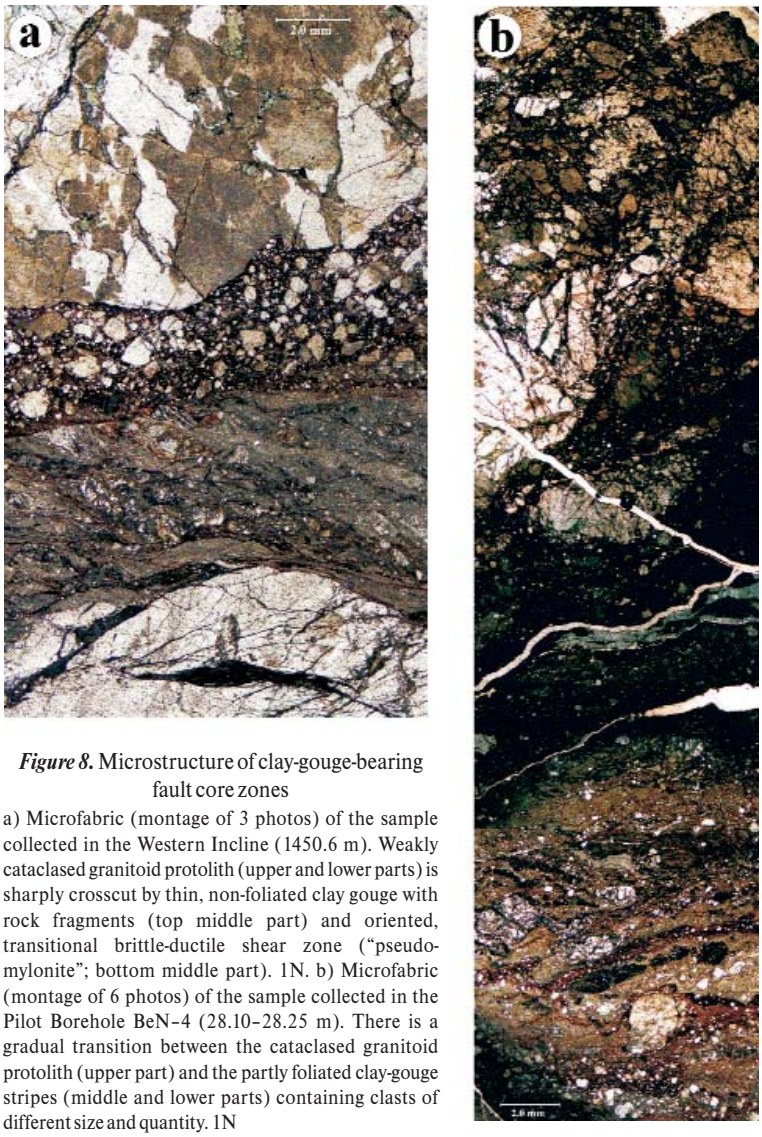

Figure 8. Microstructure of clay-gouge-bearing fault core zones

a) Microfabric (montage of 3 photos) of the sample collected in the Western Incline (1450.6 m). Weakly cataclased granitoid protolith (upper and lower parts) is sharply crosscut by thin, non-foliated clay gouge with rock fragments (top middle part) and oriented, transitional brittle-ductile shear zone ("pseudomylonite"; bottom middle part). 1N. b) Microfabric (montage of 6 photos) of the sample collected in the Pilot Borehole BeN-4 (28.10–28.25 m). There is a gradual transition between the cataclased granitoid protolith (upper part) and the partly foliated clay-gouge stripes (middle and lower parts) containing clasts of different size and quantity. 1N

8. ábra. Vetőagyagos magzónájú törészónák mikroszerkezete

a) A Nyugati lejtősakna 1450,6 méterében gyűjtött minta szöveti képe (3 vékonycsiszolati fotóból összeállítva). Alul és felül a gyengén kataklázosodott granitoid-protolit, amelyet éles határral vékony, nem foliált, kőzettörmelékes vetőagyag (felül) és irányított szerkezetű átmeneti képlékeny-töréses nyírózóna („pszeudomilonit"; alul) szel át. 1N. b) A BeN-4 fúrás 28,10–28,25 méteréből vett minta áttekintő szöveti képe (6 vékonycsiszolati fotóból összeállítva). A kataklázosodott granitoid-protolit (felül) és a változó mennyiségű és méretű klasztot tartalmazó, részben foliált szerkezetű vetőagyagsávok (középen és alul) között fokozatos átmenet észlelhető. 1N

Mineralogical Composition of Clay Gouges Deriving from Fault Core Zones

The mineralogical composition of clay gouges collected from fault core zones is characterised by the illite-smectite-mixed-layer illite/smectite-chlorite-palygorskite-kaolinite-quartz-K-feldspar-plagioclase-calcite-dolomite assemblage with highly various proportion of the individual phases according to the results of numerous XRD, TA and thin section investigations. Hematite, goethite, siderite, anatase, amphibole and pyrite occur in subordinate quantities (<5 wt%) only (for details see MAROS, KOROKNAI 2009). The quantity of the individual phases can strongly vary in samples taken from different localities of the same fault zone. This is partly due to the local inhomogenities in the intensity of protolith alteration, partly to the change of the primary rock type of the protolith. The proportion of phyllosilicates (clay minerals+chlorite) varies generally between 30–70 wt%, that of quartz+feldspars amounts mostly 20–50 wt%. The proportion of carbonates usually

varies between 7–15 wt%, but in some cases it reaches even 40 wt%. Among the clay minerals the most frequent ones are illite and smectite (up to almost 40 wt%). It is common phenomenon that a certain fault zone is characterised by the predominance of one of them. Chlorite is the third most important phyllosilicate, its proportion varies generally between 5–15 wt%, but locally exceeds 20 wt%. Kaolinite and palygorskite appear only locally, their proportion is usually low (<10 wt%), although quantity of palygorskite can reach exceptionally even 20 wt% (e.g. certain samples of the Patrik Fault).

From the above mineral assemblage clay minerals and chlorite are clearly the products of mineral transformations of the protolith caused by intense fluid flow, while K-feldspar and plagioclase represent the relict phases of the granitoid protolith. Quartz can form both relict and neoform phase. Carbonates (calcite, dolomite, and siderite) are clearly neoform phases precipitated from fluids. Thus, the high proportion of clay minerals+chlorite (>50–60 wt%) indicates intense alteration of the host rock, while the relatively high proportion of quartz+feldspars (>40 wt%) mostly suggests a smaller degree of alteration. The considerable amount of carbonates is not necessarily associated with intense clayey rock alteration.

The Map-scale Pattern of the Fault Zones

The *map-scale pattern* of the fault zones and the important individual faults in the tunnels and their close vicinity is shown in Figure 9. The map has been projected to the 2 m level plane in the tunnels. The dip of this plane is about 10% along the inclines (≈1750 m) that means about 5.7°. The altitude of the projection plane is 155 m at the entrances and reaches 0 m by the end of the inclines.

The reliability of the map is guaranteed by the continuous presence of geologists and the fairly cautiously designed mapping methods (Gyalog et al. 2010), but at the same time, the detailed mapping of the fault zones became difficult in a number of cases or became impossible in a few cases precisely because of safety reasons.

Basically two types of brittle structural elements are distinguished on the tunnel map. The individual but in this scale still distinctive faults are marked by black, the fault zones that can be correlated are marked by red in tunnel areas and green in deep borehole and exploratory trench areas. The red individual fault zones correspond to the characteristic boundary faults of zone sections that show the most significant deformation, fault gouge(s) in numerous cases, in the fault zone (master faults if core zone is present). The determined kinematics along the individual zones and the correlated faults is indicated near the relevant elements. These data have been measured on the given plane or on elements of a fault bundle and their near vicinity (1-2 m distance).

It can happen that a blackly marked fault continues in a red fault zone. The reason for this can be either the lack of adequate number of observations or the natural termination of the fault zone. The fault zones in the ground-based deep boreholes and pilot boreholes have been plotted on the projection plane with the measured dip direction. All three, differently coloured data groups have been correlated. The so-called "superzones" of fault zone bundles (numbered between 1–20) that can be correlated to the largest distances have been separated. The correlation naturally also includes conceptual elements, since the individual faults and fault zones can be connected only with a certain probability between the tunnels (25-50 m) and between the boreholes, exploratory trenches and tunnels (≈100-200 m). For the correlation between the tunnels it was supposed that—generally within a few m-zone—the individual faults and fault zones form a braiding (see Figure 3). The reliability of the correlation is supported by the structural experience obtained during the borehole exploration (Maros et al. 2003) and the mapping (Gyalog et al. 2006) of the area, the structural model compiled on the grounds of them (Maros et al. 2004, Maros 2006) and the observations about the relation among the structural elements in the tunnels. The correlation was supported by 3D modelling (Maros et al. 2009). Although the correlation of hydrogeology with the structural elements is not subject of this paper, the zones showing the greatest hydrogeological damming-isolating zones, zone-bundles are coloured purple.

Fault zones can be considered fairly frequent structural elements in the research area if the experience of the 1:10 000 scale geological-structural mapping in the NE part of the Mórágy Block (Gyalog et al. 2006) and the observations in the tunnels are taken into consideration. On the basis of the introduced map and the structural observations in the environment (Maros, koroknai 2009) it can be stated that the distance between the first-class (several m thick, distinctly traceable longitudinal, generally with clayey core zone), mostly NE–SW striking (so-called longitudinal) and E–W striking fault zones is about 500 m, while the distance of zones of less importance is approximately 50–100 m in this smaller (≈2×3 km) segment of the Mórágy Granite. The presently available data are not enough to take sides whether the above observations can be considered valid for the whole pluton.

Dip Distribution of the Fault Zones

There is a problem of how to choose the concrete fault(s) that represent(s) most precisely the spatial situation of the whole complex fault zone, which contains numerous faults of different orientation, during the determination of the *orientation of fault zones.* According to authors' experience, the generally fairly distinct master faults that border the clayey core zones can be considered the most certain reference. So the orientation of the metre(s)-thick, more significant fault zones was determined from the orientation of the master faults (or for lack of them: the characteristic faults) during the documentation of the outcrops,

exploratory trenches and tunnels in the area. If the master faults were undulating, the average of their orientation was taken. In the case of the orientation of fault zones crossed in the tunnels, an excellent independent control was offered by the correlation between the tunnels running parallelly close to each other, besides the in situ structural measurements. The situation is much more complicated in the case of the boreholes, since core recovery is usually insufficient from fault zones, so complex methods are needed to be applied here (MAROS et al. 2003, MAROS 2006, ZILAHI 2000), but the determination of the orientation was possible also with the help of master faults.

The orientation of altogether 323 fault zones was determined in the research objects of different types. The ground-based boreholes and the tunnels represent about the same quantity of data (101 and 133 respectively), while 58 zones were documented in outcrops and 30 in exploratory trenches. The steep, longitudinal (approximately NE–SW striking), mainly NW dipping fault zones are predominant in the total distribution (Figure 10, a), while the secondary maximum is represented by nearly vertical, E–W striking, mostly S dipping zones. Besides, a tertiary—rather blurred—maximum is given by NW–SE striking (so-called transversal), generally steep NE dipping fault zones. Finally, N–S striking zones occur relatively subordinately, they are partly steep (60–80°), partly quite low-angled (30–50°) and dip mostly to W. The primary maximum is given also by NE–SW striking (mainly NW dipping) zones (Figure 10, b) in the *ground-based boreholes*. The E–W and N–S striking fault zones are substantially less important. The subordinate role of transversal (NW–SE) fault zones is remarkable. In the *outcrops* the main maximum is also given by approximately longitudinal fault zones, half of which dipping to SE, half to NW (Figure 10, c). The longitudinal, rather blurred maximum is distinctly visibly made up of two submaxima: a WSW–ENE (mostly SSE dipping) and a NNE–SSW striking maxima. Not much behind the longitudinal primary maximum succeeds the transversal fault zones with rather scattered dip directions and steep NE dip. To sum up, it can be stated that the main maxima of the fault zones observed in the boreholes and outcrops situated in a fairly large area reflect the two most important orientations of individual faults (BALLA et al. 2008: Figure 155).

The distribution of the fault zones in the *exploratory trenches* (Figure 10, d), which refer to substantially smaller subareas, also the steep, approximately longitudinal zones predominate as a whole, but the transversal zones with rather scattered dip directions are also important. At the same time, the distribution patterns of the two exploratory trenches are strikingly different, they completely follow the distribution patterns of the individual faults (BALLA et al. 2008: Figure 155). While NE–SW striking, mostly SE dipping and about perpendicular (N)NW–(S)SE striking zones rule in Trench A1, in Trench A2 approximately ENE–WSW striking fault zones dominate with NW dip direction with NW–SE and E–W striking ones also appearing in smaller number.

Two, roughly equivalent maxima can be noticed in the distribution of fault zones mapped in the *tunnels* (Figure 10, e). The most striking maximum is shown by approximately E–W striking, mostly S dipping zones with longitudinal, NW dipping fault zones, parallel to the Mecsekalja Zone, lagging slightly behind. The transversal (NNW–SSE striking), mainly steeply ENE dipping fault zones give a smaller but still significant maximum. NW–SE striking fault zones cannot be distinguished as a separate maximum in the stereogram, the fault zones belonging to this group "hide" in the "blurred" maxima of the NNW–SSE striking fault zones. Finally, a steep (60–80°) and a low-angled (35–60°) group,

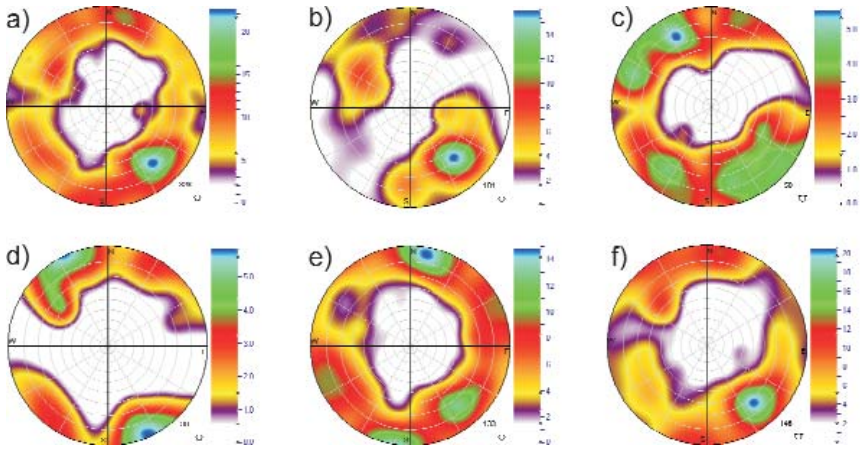

Figure 10. Pole distribution diagrams of fault zones

a) total distribution, b) ground-based boreholes, c) outcrops, d) exploratory trenches, e) tunnels (together with the pilot boreholes), f) clay-gouge-bearing fault zones; the stereograms are in lower hemisphere projection; in the bottom right corner of the stereograms the number of data is displayed

10. ábra. Törészónák pólussűrűségi diagramjai

a) összesített eloszlás, b) felszíni fúrások, c) feltárások, d) kutatóárkok, e) lejtősaknák (a vágatfúrásokkal együtt), f) vetőagyagos magzónával rendelkező törészónák; a sztereogramok alsófélgömb-vetületben készültek; a sztereogrammok jobb alsó sarkában az ábrázolt adatok száma látható

both of about N–S strike appear with less significant maxima.

As was mentioned earlier, the individual, smaller fault zones, observed in the tunnels, can usually be treated as parts of a greater "*superzone*". Out of the such created 20 "superzones" (Figure 9) 7 are longitudinal and 7 transversal, 4 are E–W and 2 are N–S striking. The approximately longitudinal and transversal "superzones" both can be further divided into two subgroups: the longitudinal ones into subgroups with a ENE–WSW (4) and a (N)NE–(S)SW (3) strike, the transversal ones into subgroups with a NNW–SSE (5) and a WNW–ESE (2) strikes. The significance of this geometry—which, as it was seen, can be recognised in the distribution picture of the individual fault zones documented in the different research objects—will be discussed at the kinematic evaluation of the fault pattern.

Because of their structural importance, the distribution of the *clay-gouge-bearing fault zones* (Figure 10, f) was examined separately besides the distribution of the fault zones occurring in the different exploration objects. The main maxima in their distribution pattern and their succession basically agree with that of all fault zones: longitudinal zones (about NE–SW) predominate with the other main orientations characteristic of the area (E–W, transversal, N–S) being also present. The secondary and tertiary maxima, however, are noticeably smaller than in the distribution of all fault zones. In other words: longitudinal fault zones are considerably more frequent among the clay-gouge-bearing fault zones than among all the zones. This throws light on the fact that the approximately NE–SW direction played a prominent role also during the brittle deformation, as it was determinative during the magmatic and ductile structural evolution of the Mórágy Block.

If the spatial orientations of the above discussed *fault zones of different orders* (Figure 5) are compared, similar characteristic features can be recognised: longitudinal zones clearly predominate in all distributions, and besides, the approximately E–W striking, the transversal (approximately NW–SE striking) and the approximately N–S striking fault zones appear everywhere. Differences appear first of all in the relative significance of the secondary and tertiary maxima, as well as in their succession. It is worth mentioning that the N–S zones play a subordinate role among the significant zones.

The following fault groups can be regarded as determinant in the brittle model of the exploration area on grounds of all these data and the several ten thousand individual faults:

Longitudinal (about NE–SW, ±10°), commonly 70–85° dipping planes approximately parallel to the magmatic and metamorphic structures of the area, with ENE–WSW striking planes being also important.

Transversal NW–SE and NNW–SSE striking, nearly vertical fault systems that probably crosscut the longitudinal fault system.

E–W and ESE–WNW striking nearly vertical fault system. In the tunnels this direction is more frequent in the distribution of faults bearing slickenlines than in that of individual faults.

The N–S fault system has subordinate importance. The dip angles significantly vary here. Nearly vertically dipping zones and faults occur, but a low-angled, 35–55° dipping group is also characteristic.

There are also local distribution patterns besides the above mentioned generally characteristic fault pattern, where certain maxima are locally stronger. This indicates that smaller deformation units (structural domains) developed in the area. For example, the difference between local distribution patterns can be distinctly noticed in the data of the two exploratory trenches, which represent quite small areas. Such is the case with the E–W strike maximum of the fault zones in the environment of Kismórágy and in the quarries near Mothers' Spring (Anyák-kútja). The total picture of the tunnels (Balla et al. 2008: Figure 250) which were mapped in about 2 km length, is also put together of smaller (a few 100 m) significantly differing blocks: transversal faults and fault zones predominate in the first 400 m, the E–W striking system dominates between 400 and 650 m, the longitudinal system appears spectacularly between 650 and 1250 m, an E–W striking system can be observed down to the end of the inclines (approximately 1700 m), then again longitudinal and transversal structures appear in the horizontal tunnels of the so-called Small Loop and Large Loop. So, in this sense, even the fault system of the tunnels, which represent a rather small area, varies and can be divided into subsystems. The general characteristic features in the distribution of faults within a relatively small rock body compared to the whole pluton can be extended to the whole granite body only if it is assumed that the brittle structures have a fractal distribution.

Kinematic Model of the Fault Zones

The determination of the kinematics of the displacements in fault zones was impossible in most cases for want of slickenlines and other markers showing the direction of the displacement. The character of displacement could be determined (with more or less certainty) in about third of the fault zones (Balla et al. 2008: Appendix VIII). As for the amplitude of the displacements, it is extraordinarily difficult to quantify it because of the amount of identifiable markers being negligible. Where markers occurred (usually leucocratic dykes), dm-sized displacements seemed to be the most common, and sometimes metre-sized displacements could be suspected. Nevertheless it can be assumed that substantially larger (several 10s m, maybe about 100 m) displacements could accumulate in certain fault zones, but no direct observation is at hand concerning this. To determine the maximum displacement, however, can be continued by the fact that no visible displacement affected the Mecsekalja Zone (at least in map scale); this indicates that no significant displacement happened along fault zones, striking NW–SE, NNW–SSE, N–S, that close great angles with the Mecsekalja Zone

The slickenlines measured in the ground-based deep boreholes and outcrops had been evaluated in a previous work (MAROS et al. 2004) in detail and 10 paleo-stressfields had been separated. Although the number of measured slickenlines has increased largely during the explorations done since then, only slickenlines and displacements closely connected to the fault zones in this paper are discussed. The kinematic model of the displacements and the origin of the fault zone pattern are outlined with brittle phases much less than earlier on grounds of the significant structural directions. It must be stressed that the following train of thought is based purely on geometrical considerations. The principle of Ockham's razor will be followed, which states that the simplest adequate solution has to be strived for.

The starting-points are the following:

1. The dip angle of the fault zones is steep in most cases.

2. The fault zones constitute braids, deformation lenses, sigmoids, geometrically strike-slip duplexes.

3. Most of the slickenlines show strike-slip or oblique strike-slip character; in the latter group oblique inverse slickenlines occur frequently.

4. Several slickenlines, often of opposite characters could be observed within a zone or even on the same fault plane, so faults could be multiply reactivated.

5. Most of the presently observable slickenlines were presumably formed during the younger movements.

6. The granite pluton is considered as a rather rigid body compared with its environment; this means that in spite of the fact that the direction of the stressfield changes, the renewal of old faults involves less energy investment than the creation of new ones.

It follows that the kinematic evolution history of the area has to be modelled basically by strike-slip and in at least one phase transpressional strike-slip stressfields.

The planes bearing the measured slickenlines can be seen in Figure 11 according to their character.

Sinistral and oblique sinistral slickenlines (Figure 11, a) were measured mostly in the longitudinal, subordinately in the N–S striking zones. The distribution of dextral slickenlines (Figure 11, b) shows a more various picture (no oblique dextral slickenlines occur): all main directions can be found, but the longitudinal direction predominates again. I the distribution of normal slickenlines (Figure 11, c) the longitudinal and transversal planes dominate, but the N–S striking ones are also important with the E–W planes being subordinate. It is striking in the distribution of the inverse and oblique inverse displacements (Figure 11, d) that transversal planes are missing, and the N–S and E–W striking planes appear besides the longitudinal ones. The distributions clearly show that displacements of opposite character could often happen along planes of the same orientation, this is illustrated by Figure 11, e, which shows zones containing different slickenlines. This is the unambiguous proof of the renewal of the fault zones. It has to be stressed again that deformation took place along undulating, lenticular-sigmoidal planes, so local normal and inverse faults have to be taken into account, oblique strike-slips along bended surfaces despite the fact that the main displacement was horizontal along the zone. The brittle deformation caused by cooling during the intrusion of the pluton and the stressfields that controlled the intrusion of the leucocratic dykes and formed the foliations and folds are not discussed in this paper, these had been discussed in previous papers (MAROS et al. 2003, KOROKNAI 2003, MAROS et al. 2004, MAROS 2006, KOROKNAI 2009) in detail. All these deformations preformed the deformations of subsequent phases. It seems probable, for example, that the pure shear and simple shear stressfields resulting in the foliations had left brittle deformation after them, too and caused—if NW–SE pressure is assumed—≈N–S sinistral, ≈WNW–ESE dextral displacements besides NW–SE normal and NE–SW inverse faults.

The clockwise rotation of the Tisza Unit in the Tertiary has to be taken into account during the discussion of the brittle deformation history by all means. According to palaeomagnetic data, MÁRTON and MÁRTON (1999) determined an average 60° for the rotation. The mutual geodynamic influence of the rotation and the Tertiary (Neogene) stressfields on the wider environment (Mecsek–Villány, Pannonian Basin) has been analysed in several works (CSONTOS et al. 1991, FODOR et al. 1999, CSONTOS et al. 2002b), and a number of stressfield were

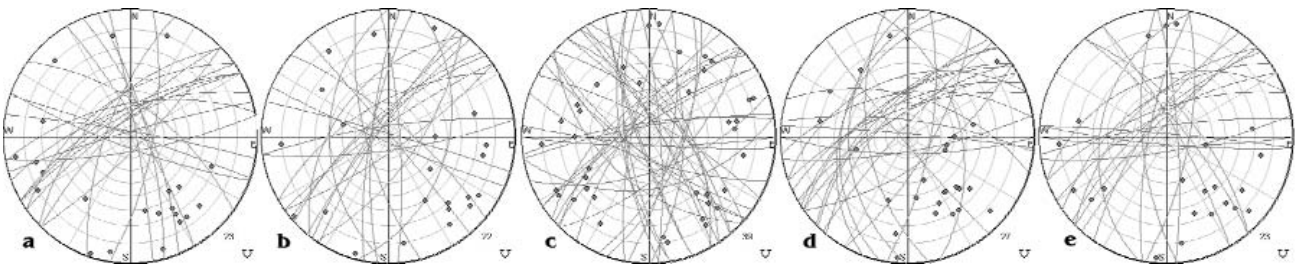

Figure 11. Fault planes with slickenlines in the fault zones and their close vicinity

a) sinistral, oblique sinistral, b) dextral, c) normal, oblique normal, d) inverse, oblique inverse, e) fault planes bearing various slickenlines; the stereograms are in lower hemisphere projection; in the bottom right corner of the stereograms the number of data is displayed

11. ábra. Vetőkarcok síkjai a törészónákban és közvetlen közelükben

a) balos, ferde balos, b) jobbos, c) normál, ferde normál, d) inverz, ferde inverz, e) többféle vetőkarcot tartalmazó síkok; a sztereogramok alsófélgömb-vetületben készültek; a sztereogrammok jobb alsó sarkában az ábrázolt adatok száma látható

determined, especially on grounds of structural examinations in sedimentary rocks, in these works. The time separation of the individual brittle phases cannot be done directly in this case, and the Mesozoic phases are not discussed in the above works, so their results are treated as analogous data that help refine the model, and the identification of the phases with the structural evolution of the granite pluton cannot be certainly done. So in this paper a much simpler (Figure 12) model has been worked out, which can be looked upon as a structural frame for more elaborated stressfield analyses, including the possible further development of an earlier work (MAROS et al. 2004).

The post-ductile structural model is based fundamentally on two main deformation phases (Figure 12, a and c, cf. Figure 9 and 11). Both deformations are dextral strike slips, the later developed in transpressional stressfield. The progressive strike-slip structure in Figure 12, a-n is supposed to be older (Phase 1), it is supposedly Mesozoic. The model explains the most characteristic, longitudinal fault pattern in the area with great reliability. The connecting P faults can be noticed in a number of cases on the map (Figure 9), and they distinctly separate from the main longitudinal planes also in stereogram (e.g. Figure 10, c). They show also dextral, oblique inverse or oblique dextral character of displacement. If they approach N–S strike direction, they are clearly inverse faults (Figure 11, d, cf. Figure 10, a and b). The antithetic Riedel faults are sinistral and do not cross the deformation lenses. The R faults joined to the S faults constitute the E–W and WSW–ENE directions with dextral displacement. In the direction of the compression and also in the tension gashes normal faults evolve with ≈30° difference compared to the E–W and WSW–ENE directions. Phase 2 is shown in Figure 12, c. Its age was determined as Tertiary but can even be connected to the recent (HORVÁTH et al. 2005) stressfield. The clockwise rotation of the area took place between the two phases (Figure 12, b). In Phase 2 the transversal NNW–SSE striking zones are considered to be the main displacement directions with dextral character; the P faults are represented by the WNW–ESE striking zones, which are also dextral. The S and R faults are represented by the bent, flattened S-shaped N–S zones, again with dextral displacement. The previously main longitudinal shear zones become antithetic Riedel faults (R') in this system with sinistral character. The nearly E–W fault zones renew as inverse or inverse dextral displacements. Normal faults appear in approximately NE–SW direction. This model covers most of the fault groups bearing slickenlines (Figure 11), the only exceptions are the N–S and E–W normal slickenlines. The former can be fit into the first, the latter into the second phase with a 20–25° error, which can be explained by the supposition of deformation lenses.

The model explains a number of so far seemingly

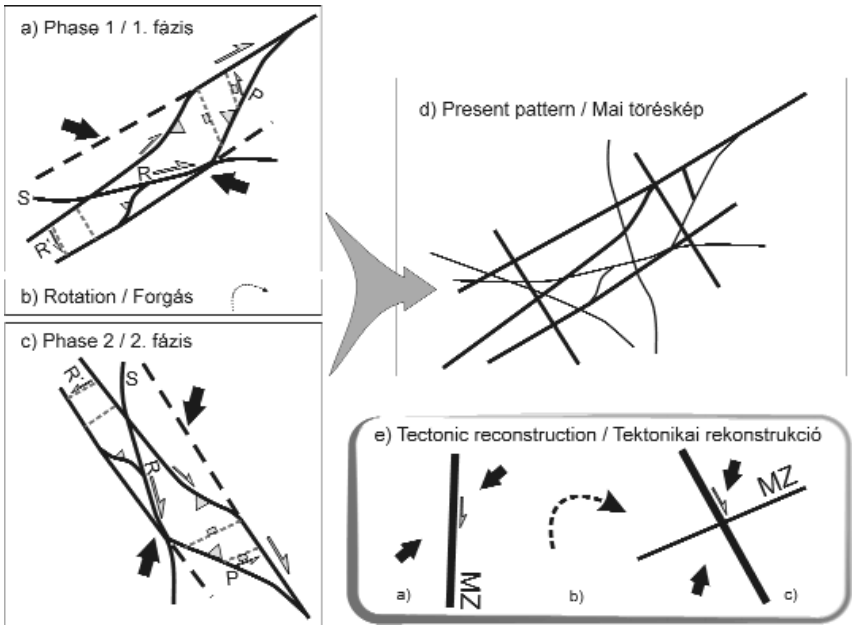

Figure 12. Kinematic model and tectonic reconstruction on grounds of the observed geometric and kinematic features of the fault zones

a) Phase 1: Variscan or Mesozoic dextral system, b) clockwise rotation, c) Phase 2: post-rotation dextral system, d) resultant fault pattern of the area, e) reconstruction of the main tectonic events; dashed arrow = rotation of the Tisza Unit, R = synthetic Riedel fault, R' = antithetic Riedel fault, P = P fault, S = splay fault, MZ = Mecsekalja Zone

12. ábra. Kinematikai modell és tektonikai rekonstrukció a törészónák megfigyelt geometriai és kinematikai észlelései alapján

a) 1. fázis: variszkuszi vagy mezozoos jobbos rendszer, b) óramutató járásával megegyező irányú forgás, c) 2. fázis: forgás utáni jobbos rendszer, d) a terület eredő törésmintázata, e) a legfőbb tektonikai események rekonstrukciója; szaggatott nyíl = a Tiszai-egység forgása, R = segítő Riedel-törés, R' = gátló Riedel-törés, P = P-törés, S = kihajló törés, MZ = Mecsekalja-öv

controversal phenomena in the area: 1) slickenlines of opposite or—according to the dip angle of the plane—surprising character on the same fault surface, 2) the renewal, as well as 3) the longitudinal zones are crosscut mainly by the transversal but even by the N–S and E–W striking faults. The two phases have resulted in a fault zone pattern (Figure 12, d), which is in good agreement with the map pattern of the fault zones (Figure 9). Figure 12, e introduces the main stages of the outlined geodynamic evolution of the area.

It should be emphasised that most probably other deformation fields have also left their marks in the area (including e.g. a longitudinal sinistral strike-slip system that would explain the orientation distribution of the Cretaceous alkaline volcanite dykes [KOROKNAI, GULÁCSI 2006]). The uplift of the Southern Transdanubian basement blocks can be supposed to happen as sinistral or compressional structures in the recent-subrecent stressfields as far as the directions of the compression and the situation of the longitudinal large zones (e.g. Mecsekalja Zone; WEIN 1965, TARI 1992, CSONTOS et al. 2002a) are known. It must be stressed that the longitudinal, clay-gouge-bearing fault zone bundles can be so "prepared" for deformation by this time that the strike-slip duplexes that are necessary for the uplift, but even the purely compressive uplifts, can be easily formed only within these zones. This leads to an important conclusion concerning the disposal of radioactive waste: the E–W striking zones have been under compression or transpression in the young and recent stressfields, so they are tightly closed for waterflow. They often crosscut the fault zones of other strikes owing to the multiple renewal and commonly have clay-gouge-bearing core zones. Taking all this into consideration, this is how the recently observable significant damming-isolating effect could have developed along certain E–W striking fault zones ("Klára", "Péter" and "Zoltán Fault"). It seems to be unimportant from hydrogeological point of view that occasionally these zones can be crosscut by other, also clay-gouge-bearing fault zones characterised with small displacements.

Another hydrogeological deduction arises. The fault that is interpreted as a P fault connected to the "Patrik Fault" is one of the most significant conductive zone. During Phase 1 and 2 opposite displacement took place along this zone. The longitudinal fault zones often close these faults—that are connecting elements between them to channel deformation—and work as terminations of the P faults at the same time. So a slight rotation happens along them during displacements, which results in openings along the P faults. This causes these faults to be conductive but only up to the joining points with the longitudinal faults. Consequently, flow is restricted sidewise and will rather follow vertical paths instead. Authors' hydrogeological conclusions are in accordance with the model of BENEDEK et al. (2009), in which waterflow takes place in a system of rock blocks that are put beside one another like mosaics, have different conductivity and hydraulically communicate only restrictively with one another.

Radiometric Dating

Illite-rich fine fractions (<10, <2, and <1 μm) were separated from clay-gouge samples deriving from most strongly deformed fault core zones, which—following the determination of the mineralogical composition by the XRD method—were analysed in the Institute of Nuclear Research (Debrecen) to obtain K–Ar age data. The results are summarised in Table 1, which also contains the previously published age data (KOVÁCS-PÁLFFY, FÖLDVÁRI 2004), as well as the polytypic variety and FWHM (full-thickness-at-half-maximum, which corresponds roughly to the so-called Kübler index; for details see GUGGENHEIM et al. 2001) values of illite as determined from the illite-rich fine fractions.

In the samples studied the polytypic variety of illite is predominantly 1M that appears relatively rarely according to the literature. Its formation is clearly connected to hydrothermal processes (PEACOR et al. 2002, HAINES, van der PLUIJM 2008). Beside the prevailing polytype 1M the subordinate presence (several wt%) of the polytype $2M_1$ can be assumed in some samples (although not to confirm unambiguously), and in two cases the polytype $1M_d$ also appears. The polytype $2M_1$ appears as a clearly identificable, separate phase (consequently in a relatively considerable proportion) only in two samples. The polytype $1M_d$ represents practically the more disordered variety (displaying fewer reflections) of the polytype 1M, its formation may be connected to the low-T alteration of the polytype 1M. The polytype $2M_1$, characteristic of metamorphic rocks, may derive from the biotite of the granitoid protolith, or from muscovite formed by the metamorphic transformation of primary magmatic biotite, although its hydrothermal origin—as well as in the case of polytype $1M_d$—is also described in the literature (LONKER, FITZ GERALD 1990).

The FWHM values of 1M illite could be determined in 9 cases of the dated 16 samples, the data scatter in a rather large range ($\Delta°2\Theta$: 0.55–1.02). In the rest of the samples (7 cases) the FWHM values of illite could not be determined separately because of the considerable amounts of mixed-layer illite/smectite (locally smectite as well). Because of the presence of overlapping peaks only a "joint" FWHM value of illite-illite/smectite (±smectite) can be obtained in these samples that range between 2.0 and 4.5. The large amount of mixed-layer illite/smectite (±smectite) may indicate the low-T transformation of primary illite.

Considering the FWHM values of 1M illite determined in 9 cases two subgroups can be distinguished: one of the subgroups contains the four samples of the borehole Üh–1 that represent also a spatially separate group of samples. The FWHM values are here relatively low ($\Delta°2\Theta$: 0.55–0.68); this suggests a discrete, practically unaltered (or only minimally altered) illite structure. These $\Delta°2\Theta$ values are characteristic of the diagenetic zone formally.

In the other subgroup (samples deriving from the boreholes Üh–2, Üh–5, Üh–22 and Bp–1) the FWHM values are considerably higher ($\Delta°2\Theta$: 0.75–1.02); this tends to show the transformation of illite.

Table 1. Overview on the K–Ar ages obtained on illite-rich fine fractions deriving from clay-gouge-bearing fault core zones, furthermore on polytypism and FWHM values of illite

Sample locality	Depth (m)	Size fraction (μm)	Poly-typism	FWHM (° 2Θ)	K (%)	^{40}Ar(rad) (cc STP/g)	^{40}Ar(rad) (%)	Measured age (Ma ± ?)	Geological age	Geological position of the sample
Borehole Üh-2	367.1-367.7	<10	1M	1.02	6.41	1.913×10^{-5}	68.7	75.2±3.0**	Late Cretaceous	transversal (50/80°), thick (≈25 m), major fault zone (superzone 20)
Borehole Üh-22	182.60	<2	1M	0.88	5.80	2.482×10^{-5}	90.2	106.9±4.1**	Early Cretaceous	longitudinal (315/60°), important (≈5 m), dextral-inverse fault zone (Tz22-7)
	278.10	<2	1M (2M)	0.98	4.35	2.047×10^{-5}	89.3	117.2±4.5**	Early Cretaceous	approx. longitudinal (340/65°), minor (≈3 m), sinistral-inverse(?) fault zone (Tz22-11)
	298.3	<1	1M 2M	–**	3.86	1.027×10^{-5}	65.9	67.1± 2.7	Late Cretaceous	"transitional" (345/75°), important (≈5 m) fault zone (Tz22-12)
Borehole Üh-5	107.03	<10	1M 2M	0.82	4.60	3.245×10^{-5}	84.8	172.9±6.6**	Middle Jurassic	minor (≈3 m) fault zone (Tz5-2) with unknown orientation
Borehole Üh-1	346.10	<2	1M ($1M_d$)	0.56	6.33	4.941×10^{-5}	88.3	190.3±7.2 **	Early Jurassic	strike-slip fault zone with unknown orientation
	343.90	<2	1M ($1M_d$, 2M)	0.68	7.27	6.285×10^{-5}	93.9	208.8±7.9**	Late Triassic	
	345.70	<2	1M	0.55	6.29	5.580×10^{-5}	95.4	215.0**	Late Triassic	
	349.90	<2	1M	0.61	7.25	6.900×10^{-5}	96.6	229.7±8.7 **	Middle Triassic	
Eastern Incline	501.2	<2	1M	–*	3.08	1.486×10^{-5}	70.4	119.9 ± 3.8	Early Cretaceous	E-W-striking (10/85°), thick (≈20 m), dextral(?), major, damming-isolating fault zone (Klára Fault, superzone 5)
	505.9	<2	1M (2M)	–**	3.56	1.835×10^{-5}	73.6	128.0 ± 4.0	Early Cretaceous	
	507.8	<2	1M (2M)	–**	1.97	1.032×10^{-5}	22.8	129.8 ± 8.0	Early Cretaceous	
	510.0	<2	1M	–**	4.74	2.835×10^{-5}	68.5	125.0 ± 4.0	Early Cretaceous	
Eastern Incline	1392.9	<1	1M	–**	2.57	9.230×10^{-6}	62.2	90.0±3.6	Late Cretaceous	E-W-striking (185/85°), thin (≈2 m), damming-isolating, sinistral(?) fault zone (Péter Fault, superzone 11)
Interconnecting Passageway 7	≈1738.5	<1	1M	–**	2.41	7.546×10^{-6}	34.1	78.7±4.0	Late Cretaceous	transversal (≈40/76°), minor (≈2 m), dextral(?) fault zone (7OK-1)
Underground Borehole Bp-1	71.4	<1	1M (2M)	0.75	4.89	3.292×10^{-6}	75.1	165.2±6.4	Middle Jurassic	E-W-striking (185/84°), minor (1-2 m) fault zone (Bp-1-2)

* FWHM values of 1M illite could not be determined separately because of the considerable amounts of illite/smectite, ±smectite. (Formally: Δ° 2Θ> 2,0).

** Data published by KOVÁCS-PÁLFFY, FÖLDVÁRI (2004). (2M), (1Md): Assumed polytype present only in subordinate quantity (several wt%).

K–Ar ages obtained on illite-rich fine fractions are exclusively Mesozoic, most of them (10 cases of the 16 samples) belongs to the Cretaceous, furthermore there are also three Triassic and three Jurassic ages (Table 1). The K–Ar ages display a clear younging trend with the increasing FWHM values of illite (Figure 13). This relationship is unfortunately not to study in the case of those 7 samples (deriving from the Eastern Incline, Interconnecting Passageway 7 and the Borehole Üh–22), which exhibit extremely high FWHM values ($\Delta°2\Theta>2.0$). These samples define a separate group, where only a "joint" FWHM value of illite–illite/smectite (±smectite) can be obtained.

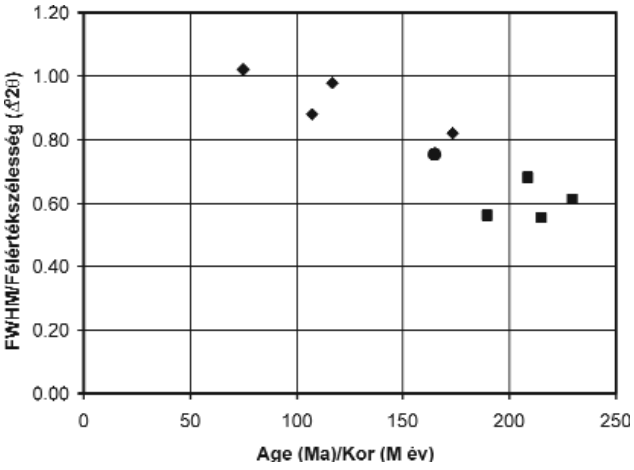

Figure 13. Relationship between K–Ar ages on illite-rich fine fractions and FWHM values of illite
Square = Üh–1, circle = Bp–1, rhomb = Üh–2, Üh–5, Üh–22

13. ábra. Az illitdús finomfrakciókban meghatározott K–Ar-korok és az illit-félértékszélességek kapcsolata
Négyzet = Üh–1, kör = Bp–1, rombusz = Üh–2, Üh–5, Üh–22

Considering the results from an analytical point of view, the followings must be encountered:

—The most reliable ages are those ones in the case of which the samples contain discrete illite, furthermore there is no (or only negligible amounts of) mixed-layer illite/smectite or smectite.

—In the samples containing considerable amounts of mixed-layer illite/smectite, the geological meaning of the K–Ar ages is uncertain, since the exact genetics of mixed-layer illite/smectite can not be resolved by the XRD method. If the mixed-layer illite/smectite was formed by the low-T degradation of illite, the ages obtained are probably mixed ages, since the K–Ar system does not represent a closed system during this transformation. If the mixed-layer illite/smectite represents a cogenetic phase formed by the same process as 1M illite, the ages obtained are theoretically reasonable; this can have also important geological meaning. However, this possibility seems to be less probable from a mineralogical point of view.

—Finally, the age data of the samples containing considerable amounts of smectite are also somewhat problematic, since smectite may also represent a low-T alteration product of illite based on the continuous transformation series of illite > mixed-layer illite/smectite > smectite.

Based on these considerations the oldest, Middle Triassic – Early Jurassic (230–190 Ma) ages seem to be the most reliable ones from the available dataset, which all come from the Borehole Üh–1. These ages show a rather good agreement with zircon and titanite fission track ages (with a closure temperature of ca. 200 °C) deriving from different compositions of the Mórágy Granite (240–210 Ma; DUNKL 1990). Very similar Middle and Late Triassic K–Ar ages (241–198 Ma) were obtained on numerous whole rock samples of the Lower Permian Gyűrűfű Rhyolite in the wider geological surroundings (BARABÁS-STUHL 1988). Recent K–Ar, Ar–Ar and Rb–Sr investigations on mineral separates deriving from different rock types of the crystalline basement of the Tisza Unit yielded also Middle and Late Triassic ages in several localities (LELKES-FELVÁRI et al. 2003, BALOGH et al. 2009). Similar ages (250–220 Ma) correlated with the Triassic extension were published from the Late Variscan Muntele Mare granite pluton (?295 Ma) in the Apuseni Mts. forming the eastern continuation of the Tisza Unit (ANTON 2000, BALINTONI et al. 2010). Such an age (229 Ma) was obtained for the syenitic intrusive phase of the Ditró Alkaline Massif (Eastern Carpathians) based on recent U–Pb dating of zircons (PANA et al. 2000). According to the overview of STRUTINSKI et al. (2006)—including almost 600 K–Ar ages—the Middle and Late Triassic ages are rather widespread in the Intra-Carpathian region of Romania. The regional importance of Middle to Late Triassic event(s) is also shown by the fact that they are not restricted to the Tisza Unit only, but also appear in the Pelso Unit (e.g. certain clayey altered zones within the Velence Granite: BENKÓ 2006; Telekesoldal Rhyolite of the Rudabánya Mts.: KÖVÉR SZ., pers. comm.). Based on these data the Middle and Late Triassic ages seem to represent important proofs a regional—although in details still not well-understood—geological event(s) associated with elevated heat and fluid flow, which affects the whole Intra-Carpathian region according to the available data.

From an analytical point of view two other samples (Potential Borehole Bp–1: 165 Ma – Middle Jurassic; furthermore the borehole Üh–2: 75 Ma – Late Cretaceous) containing only minor quantity of mixed-layer illite/smectite and smectite can be also qualified as samples with relatively good age data. The remaining Jurassic and Cretaceous ages can be accepted as an approximate age of tectonic activity associated with hydrothermal circulation only in that case, if one assumes that the considerable quantities of mixed-layer illite/smectite and smectite are fully cogenetic phases with 1M illite, furthermore there was absolutely no Ar loss in the mixed-layer illite/smectite. If these phases represent, however, the low-T alteration products of 1M illite, or eventually the products of a separate, lower temperature hydrothermal phase, the K–Ar ages measured are mixed ages, which are surely younger than the formation of 1M illite.

The genetics of illite plays a fundamental role in the interpretation of K–Ar ages, whereas two basic modes can be distinguished:

1) illite precipitates directly from migrating fluids, in other words: veins and fractures infilled by illite do not derive from the alteration of the neighbouring host rock,

2) illite is formed by the fluid-driven, intense in situ transformation of the rock-forming minerals—first of all: feldspars—of the granitoid host rock, in other words: illite is an authigenic phase in clay-gouge-bearing fault core zones.

The introduced microstructural, mineralogical-petrological, furthermore geochemical (NÉDLI, SZABÓ 2007) features of the samples studied clearly argue for the second mechanism. Considering the temporal relationship of the formation of illite and the age of deformation producing the fault zones studied, there are further two possibilities in the second case:

2a) In the first scenario the clayey alteration indicating intense fluid flow is not related to a particular deformation phase. The clayey alteration occurs along pre-existing weakness zones (e.g. fractures, cataclastic zones) of the granite body causing here considerable alteration in the host rock, and the subsequent deformation postdates the alteration process. This means that radiometric ages determined on illite-rich fine fractions record only the time of mineralogical transformation (illitisation due to fluid-rock interaction) in clay-gouge-bearing fault core zones, whereas brittle deformation proceeding in the zone is—even by (ten)million of years—definitely younger. This model implicitely includes the presence of three, temporally more or less well-distinguishable, independent events: (a) early deformation without significant fluid flow (and associated illitisation), (b) in situ clayey alteration due to hydrothermal effect in the tectonically preformed zone, (c) a subsequent, deformation again without significant fluid flow (and associated illitisation).

2b) In the second scenario the fluid-driven clayey alteration and the tectonic deformation are more or less coeval, moreover mutually enhancing processes. This means that the K–Ar ages obtained on illite-rich fine fractions record not only the time of mineralogical transformation (illitisation), but also the approximate age of associated brittle deformation.

The model *2b*) might represent a geologically much more probable situation than model *2a*), since the presence of some fluids is almost sure even in the case of a shallow-buried rock body. These fluids can flow obviously by much larger probability in the zones made permeable by synchronous tectonic activity, where they cause the mineralogical transformation of crushed rock material further enhancing deformation. Taking into account the discussion above and also the results of microtectonic investigations, the syn-tectonic character of illite formed roughly coeval with the genesis of fault zones can be suggested (see also "Formation and Evolution of Brittle Fault Zones"), consequently the yielded K–Ar ages—considering the analytical point of view introduced previously as well—can be interpreted as the approximate formation age of the fault zones studied. This interpretation is also supported by the well-preserved, foliated clay gouges, since the syn-tectonic, foliated microstructure suggesting high differential stress at its formation could not have been preserved in the presence of substantial, overprinting brittle deformation(s).

In this frame of interpretation the brittle deformations producing the fault zones studied clearly belong to the Alpine orogenesis according to the radiometric age data. As mentioned above the most reliable, relatively old (Middle Triassic to Early Jurassic) ages derive from the borehole Üh–1. However, one must also take into account at the geological interpretation that the fine fractions of the samples providing here the two younger ages (190 and 208 Ma) contain also the polytype $1M_d$ (Table 1), whereas the samples exhibiting the two older ages (215 and 230 Ma) contain exclusively the polytype 1M. As the polytype $1M_d$ probably represents the low-T alteration product of the polytype 1M, therefore the two older ages are regarded as analytically more reliable among the four ages deriving from this borehole. In summary, the obtained K–Ar ages deriving from the depth interval identified as the location of an important fault zone in the geological log of the borehole (KÓKAI 1997) can be interpreted as time of illite formation and associated tectonic activity basically in the Late Triassic (Carnian). Furthermore, considering the mineralogical criteria discussed above, the presence of a Middle Jurassic (165 Ma) and a Late Cretaceous (75 Ma) tectonic event can be also assumed. The tectonic meaning of the remaining, mostly Early Cretaceous ages is still questionable, although they theoretically could be fit well into the geological evolution model of the study area considering also the available data on the Cretaceous tectonics of the wider geological surroundings (e.g. WEIN 1961, 1967; NÉMEDI VARGA 1983; BENKOVICS 1997). However, it can be stated on the basis of new data that the Mórágy Granite was affected by important fluid-rock interactions associated with the formation of illite several times during the Mesozoic, which were at least partly also roughly coeval with tectonic activities.

Finally it should be also mentioned that the comparison of the available K–Ar ages and the kinematic model leads to the conclusion that the second phase of the kinematic model ranked into the Neogene was not accompanied by substantial, illite-producing rock alteration, but this phase was characterised by the reactivation of pre-existing, weak fault zones formed during the Mesozoic according to the K–Ar ages.

Formation and Development of Fault Zones

The evolution mechanism of clay-gouge-bearing fault core zones represents an important problem. On the basis of authors' field experience and their data deriving from the examination of clay fault gouges, as well as considering the relating professional literature, it can be concluded that the

formation of the core zones in question happened in the presence of fluids, simultaneously with tectonic deformation and comminution (VROLIJK, VAN DER PLUIJM 1999, JEFFERIES et al. 2006). Mineral alteration as a consequence of the presence of fluids (argillation)—in the protolith that can be ground even down to the fraction size of clay minerals (MONZAWA, OTSUKI 2003)—and tectonic deformation are mutually enhancing (positive feedback) subprocesses in this process. Tectonic strain and the brittle crumbling of mineral grains (STEWART et al. 2000) start the process during which weakened zones develop in the granite body, mainly along former weakened zones, that are well permeable also for fluids. Such weakened zones are represented either by rock boundaries, or by pseudo-mylonites (Figure 6, a) and mylonites. Deformation is assisted by the presence of fluids that quasi "soften" the shear zones. In the presumable multiply reactivated zones (which contain previously developed infillings at places) alteration triggered by fluids prevails during the deformation and its short intervals. This alteration further weakens the rock, since the newly formed, fine-grained phyllosilicates that evolve at the expense of the protolith considerably reduce the shear stress of the rock in the given zone. Consequently, the deformation will concentrate more and more into the altered zone and its environment as the process advances. This leads to the formation of newer faults and further tectonic comminution in the weakened zones that are saturated with fluids. The self-fortifying process succession finally leads to the enlargement (thickening) of the zone, the concentration of deformation and the more and more intensive mineral alteration. The final stage of the deformation process is indicated by the formation of foliated clay fault gouge (CHESTER, LOGAN 1986, LIN 2001), in which the deformation is primarily realised by the so-called cataclastic flow (ENGELDER 1974).

The fluids cannot only cause the alteration of the original rock-forming minerals (feldspars, biotite, amphibole), but other new minerals (mainly carbonates and quartz) can precipitate in new fractures that are constantly developing during the deformation as the described process advances. These infillings can break up during the progressive deformation and can mix with the mineral and rock fragments of the host rock then can be recemented or can be incorporated into the clay gouge.

Acknowledgements

The commission that constituted the base of the interpretation has been given to the Geological Institute by Puram and the Mecsekérc Plc, these results could not have been obtained without it. The authors thank all tunnel-mapping and borehole-logging geologists (Gáspár Albert, Ambrus Barabás, István Bíró, János Borsody, György Don, Márton Fórián-Szabó, Judit Füri, Zoltán Gulácsi, Pál Gyarmati, Amadé Halász, Botond Kemény, Edit Király, András Kókai, Balázs Koroknai, Zoltán Lantos, Árpád Magyari, Péter Majoros, Balázs Musitz, István Oláh, Klára Palotás, Zsolt Peregi, Géza Szebényi, Patrik Török and István Zsámbok) for their work of years, which provided the major part of the data used for the preparation of this paper. The authors thank Zoltán Balla and László Gyalog as leaders of the project to open the door to reach authors' results. The authors thank Antonyina Dudko for her pioneer work to gain knowledge about the fault zones. The authors thank Mecsekérc Plc and its subcontractors, the miner colleagues to provide the necessary place and time for the observations. The authors thank Gyula Konrád for the revision of this paper, his useful remarks.

References — Irodalom

ANTON, D. C. 2000: *Petrographical, geochemical and isotopic study of Mt. Mare granitoids, North Apuseni Mountains. PhD Thesis.* — Tokyo University, Tokyo, 163 p.

ÁRKAI, P., BALOGH, K., DEMÉNY, A., FÓRIZS, I., NAGY, G., MÁTHÉ, Z. 2000: Composition, diagenetic and post-diagenetic alterations of a possible radioactive waste repository site: the Boda Albitic Claystone Formation, southern Hungary. — *Acta Geologica Hungarica* 43 (4), pp. 351–378.

BALINTONI, I., BALICA, C., CLIVETI, M., LI-QIU, L., HAHN, H. P., CHEN, F., SCHULLER, V. 2010: The emplacement age of the Muntele Mare Variscan granite (Apuseni Mountains, Romania). — *Geologica Carpathica* 60 (6), pp. 495–504.

BALLA, Z. 2004: General characteristics of the Bátaapáti (Üveghuta) Site (South-western Hungary) (A Bátaapáti [Üveghutai]-telephely általános jellemzése). — *A Magyar Állami Földtani Intézet Évi Jelentése 2003,* Budapest, pp. 73–91.

BALLA, Z., GYALOG, L. 2009: A Mórágyi-rög északkeleti részének földtana. Magyarázó a Mórágyi-rög északkeleti részének földtani térképsorozatához (1:10 000) (Geology of the North-eastern part of the Mórágy Block. Explanatory notes to the geological map-series of the North-eastern part of the Mórágy Block [1:10,000]). — *Magyarország tájegységi térkép-sorozata (Regional map series of Hungary).* Magyar Állami Földtani Intézet, 2009, 283 p. (216 p.)

BALLA Z., ALBERT G., CHIKÁN G., DUDKO A., FODOR L., FÓRIÁN-SZABÓ M., FÖLDVÁRI M., GYALOG L., HAVAS G., HORVÁTH I., JÁMBOR Á., KAISER M., KOLOSZÁR L., KOROKNAI B., KOVÁCS-PÁLFFY P., MAROS GY., MARSI I., PALOTÁS K., PEREGI ZS., RÁLISCH L.-NÉ, ROTÁRNÉ SZALKAI Á., SZŐCS T., TÓTH GY., TURCZI G., PRÓNAY ZS., VÉRTESY L., ZILAHI-SEBESS L., GALSA A., SZONGOTH G., MEZŐ GY., MOLNÁR P., SZÉKELY F., HÁMOS G., SZŰCS I., TURGER Z., BALOGH J., JAKAB G., SZALAI Z. 2003: A felszíni földtani kutatás zárójelentése, Bátaapáti (Üveghuta),

2002–2003 (in Hungarian, translated title: Final report of the ground-based geological exploration, Bátaapáti [Üveghuta], 2002–2003). — *Manuscript (kézirat),* Magyar Állami Földtani Intézet, Budapest, Tekt. 1102; Bátatom Kft., Budapest, BA–03–156.

Balla Z., Császár G., Földvári M., Gulácsi Z., Gyalog L., Horváth I., Kaiser M., Király E., Koloszár L., Koroknai B., Magyari Á., Maros Gy., Marsi I., Musitz B., Rálisch E., Rotárné Szalkai Á., Szőcs T., Tóth Gy. (MÁFI); Berta J., Csapó Á., Csurgó G., Gorjánácz Z., Hámos G., Hogyor Z., Jakab A., Molnos I., Moskó K., Ország J., Simoncsics G., Szamos I., Szebényi G., Szűcs I., Turger Z., Várhegyi A. (Mecsekérc); Benedek K., Molnár P., Szegő I., Tungli Gy. (Golder); Madarasi A., Mártonné Szalay E., Prónay Zs., Tildy P. (ELGI); Szongoth G. (Geo-Log); Gacsályi M. (MBFH); Kovács L. (Kútfej Bt.); Mónus P. (GeoRisk); Vásárhelyi B. (Vásárhelyi és Tsa Bt.) 2008: A felszín alatti földtani kutatás zárójelentése (in Hungarian, translated title: Final Report of the underground geological research). — *Manuscript (kézirat),* Magyar Állami Földtani Intézet, Budapest, Tekt. 1419.

Balogh, K., M. Tóth, T., Dunkl, I., Scherrer, N. 2009: A polimetamorf aljzat geokronológiai viszonyai a Szeghalom és a Mezősas-Furta háton (in Hungarian, translated title: Geochronological relationships of the polymetamorphic basement on the Szeghalom and the Mezősas-Furta basement high). — *In*: M. Tóth T. (szerk.): *Magmás és metamorf képződmények a Tiszai egységben.* GeoLitera, Szeged; pp. 147–160.

Barabásné Stuhl Á. 1988: Összefoglaló jelentés a Dél-Baranyai dombság és a Villányi-hegység permi képződményeinek kutatásáról (in Hungarian, translated title: Final report on the geological research of the Permian formations of the South Baranya and the Villány Hills). — *Manuscript (kézirat),* MÉV Adattár (J–3278/IV).

Benedek, K., Bőthi, Z., Mező, Gy., Molnár, P. 2009: Compartmented flow at the Bátaapáti site in Hungary. — *Hydrogeology Journal* 17 (5), pp. 1219–1232.

Benkó, Zs. 2006: Többfázisú magmás-hidrotermális tevékenység rekonstrukciója a Velencei-hegységben (in Hungarian, translated title: Reconstruction of polyphase magmatic-hydrothermal activity in the Velence Hills). — *Abstract, Ifjú Szakemberek Ankétja, Balatonfűzfő,* pp. 28–29.

Benkovics, L. 1997: Étude structurale et géodinamique des Monts Buda, Mecsek et Villány (Hongrie). PhD Thesis. — *Manuscript (kézirat),* Universite des sciences et Technologies de Lille.

Billi, A., Salvini, F., Storti, F. 2003: The damage zone-fault core transition in carbonate rocks: implications for fault growth, structure and permeability. — *Journal of Structural Geology* 25 (11), pp. 1779–1794.

Boyer, S. E., Elliott, D. 1982: Thrust systems. — *American Association of Petroleum Geologists Bulletin* 66 (9), pp. 1196–1230.

Buda Gy. 1999: Kis és közepes radioaktivitású erőművi hulladékok végleges elhelyezése. Telephelykutatás Üveghuta körzetében. Összefoglaló jelentés az Üveghuta–22., –23. és –24. sz. fúrások granitoid kőzeteinek vizsgálatáról (in Hungarian, translated title: Summary report of the analysis of granitoid rocks from Boreholes Üveghuta–22, 23, and 24).— *Manuscript (kézirat),* Magyar Állami Földtani Intézet, Budapest, Tekt. 634.

Buda, Gy., Dobosi, G. 2004: Lamprophyre-derived high-K mafic enclaves in variscan granitoid from the Mecsek Mts. (South Hungary) — *Neues Jahrbuch für Mineralogie, Abhandlungen* 180 (2), pp. 115–147.

Buda, Gy., Puskás, Z., Gál-Sólymos, K., Klötzli, U., Cousens, B. L. 2000: Mineralogical, petrological and geochemical characteristics of crystalline rocks of the Üveghuta boreholes (Mórágy Hills, South Hungary) (Üveghutai mélyfúrások kristályos kőzeteinek ásvány-kőzettani és geokémiai jellemzése [Mórágyi-rög]). — *A Magyar Állami Földtani Intézet Évi Jelentése 1999-ről,* pp. 231–253.

Caine, J. S., Evans, J. P., Forster, C. B. 1996: Fault zone architecture and permeability structure. — *Geology* 24 (11), pp. 1025–1028.

Chester, F. M., Logan, J.M. 1986: Implications for mechanical properties of brittle faults from observations of the Punchbowl Fault zone, California. Internal structures and fault zones. — *Pure and Applied Geophysics* 124 (1), pp. 77–106.

Csontos, L., Benkovics, L., Bergerat, F., Mansy, J-L., Wórum, G. 2002a: Tertiary deformation history from seismic section study and fault analysis in a former European Tethyan margin (the Mecsek–Villány area, SW Hungary) — *Tectonophysics* 357 (1–4), pp. 81–102.

Csontos, L., Márton, E., Wórum, G., Benkovics, L. 2002b: Geodynamics of SW-Pannonian inselbergs (Mecsek and Villány Mts, SW Hungary): Inferences from a complex structural analysis — *EGU Stephan Mueller Special Publication Series* 3, pp. 227–245,

Csontos, L., Tari, G., Bergerat, F., Fodor, L. 1991: Evolution of the stress-fields in the Carpatho-Pannonian area during the Neogene. — *Tectonophysics* 199 (1), 73–91, 1991.

Dudko, A. 2000: Correlation of geological and geophysical data for the fracture zones of the Üveghuta site (Töréses övek földtani és geofizikai adatainak összevetése az üveghutai telephelyen).— *A Magyar Állami Földtani Intézet Évi Jelentése 1999-ről,* pp. 273–286.

Dudko A., Szebényi G. 2003: Jelentés az Anyák-kútja melletti kőfejtő tektonikai vizsgálatáról (in Hungarian, translated title: Report of the tectonic evaluation of the quarry near Anyák-kútja [Mothers' Spring]). — *Manuscript (kézirat),* Magyar Állami Földtani Intézet, Budapest, Tekt. 1086.

Dunkl I. 1990: A fission track módszer és alkalmazása geokronológiai kérdések megoldásában. Kandidátusi értekezés (in Hungarian, translated title: The fisssion track method and its application in the solution of geochronological problems). — *Manuscript (kézirat),* Miskolci Egytem, Miskolc.

Engelder, J. T. 1974: Cataclasis and the generation of fault gouge. — *Geological Society of America Bulletin* 85 (10), pp. 1515–1522.

Faulkner D. R., Lewis, A. C., Rutter, E. H. 2003: On the internal structure and mechanics of large strike-slip fault zones: field observations of the Carboneras fault in southeastern Spain. — *Tectonophysics* 367 (3–4), pp. 235–251.

Fodor, L., Csontos, L., Bada, G., Győrfi, I., Benkovics, L. 1999: Tertiary tectonic evolution of the Pannonian basin system and neighbouring orogens: a new synthesis of paleostress data. In: Durand, B., Jolivet, L., Horváth, F., Seranne, M. (eds): The Mediterranean Basins: Tertiary Extension within the Alpine orogen. — *Geological Society, London, Special Publication* 156, pp. 295–334.

Gerdes A. 2006: Report on the LA-ICP-MS U-Pb dating of four borehole samples from the Mecsek Mountain granitoids. —

Manuscript (kézirat), Magyar Állami Földtani Intézet, Budapest, Tekt. 1304.

GUGGENHEIM, S., BAIN, D. C., BERGAYA, F., BRIGATTI, M. F., DRITS, V. A., EBERL, D. D., FORMOSO, M. L. L., GALÁN, E., MERRIMAN, R. J., PEACOR, D. R., STANJEK, H., WATANABE, T. 2002: Report of the Association Internationale pour l'Étude des Argiles (AIPEA) Nomenclature Committee for 2001: Order, disorder and crystallinity in phyllosilicates and the use of the "crystallinity index". — *Clays and Clay Minerals* 50 (3), pp. 406–409.

GYALOG L., BALLA Z., CSÁSZÁR G., GULÁCSI Z., KAISER M., KOLOSZÁR L., KOROKNAI B., LANTOS Z., MAGYARI Á., MAROS GY., MARSI I., PEREGI ZS. 2006: Földtani és geomorfológiai térképezés jelentése (in Hungarian, translated title: Report on geological and geomorphological mapping [Üveghuta]). — *Manuscript (kézirat),* Magyar Állami Földtani Intézet, Tekt. 1339; Radioaktív Hulladékokat Kezelő Kht., Paks, RHK–K–131/06.

GYALOG L., JÁMBOR Á., KÓKAI A., MAROS GY., PEREGI ZS. (MÁFI), KONRÁD GY., MÁTHÉ Z. (Mecsekérc), SZEBÉNYI G. (Kömlődi Korrekt). 2003: A bátaapáti A1 és A2 árok földtani leírása. 1. kötet, Földtani leírás (in Hungarian, translated title: Geological mapping of the Trenches A1 and A2 at Bátaapáti. Volume 1. Geological mapping). — *Manuscript (kézirat),* Magyar Állami Földtani Intézet, Budapest, Tekt. 1000.

HAINES, S. H., VAN DER PLUIJM, B. A. 2008: Clay quantification and Ar-Ar dating of synthetic and natural gouge: Application to the Miocene Sierra Mazatan detachment fault, Sonora, Mexico. — *Journal of Structural Geology* 30 (4): pp. 525–538.

HORVÁTH, F., BADA, G., WINDHOFFER, G., CSONTOS, L., DÖVÉNYI, P., FODOR, L., GRENERCZY, GY., SÍKHEGYI, F., SZAFIÁN, P., SZÉKELY, B., TIMÁR, G., TÓTH, L., TÓTH, T., 2005: A Pannon medence jelenkori geodinamikájának atlasza: Euro-konform térképsorozat és magyarázó. OTKA T034928 sz. projekt, zárójelentés (in Hungarian, translated title: Atlas of Recent Geodynamics of the Pannonian Basin). — *Manuscript (kézirat),* ELTE Földrajz- és Földtudományi Intézet, Geofizikai Tanszék, Budapest.

JANTSKY B. 1953: A mecseki kristályos alaphegység földtani viszonyai (in Hungarian with French abstract: Les conditions géologiques du socle cristallin du Mecsek). — *A Magyar Állami Földtani Intézet Évi Jelentése 1950-ről,* pp. 65–77.

JANTSKY B. 1979: A mecseki gránitosodott kristályos alaphegység földtana (Géologie du socle cristallin granitisé de la montagne Mecsek). ľ *A Magyar Állami Földtani Intézet Évkönyve* 60, 385 p.

JEFFERIES, S. P., HOLDSWORTH, R.E., WIBBERLEY, C. A. J., SHIMAMOTO, T., SPIERS, C. J., NIEMEIJER, A. R., LLOYD, G. E. 2006: The nature and importance of phyllonite development in crustal-scale fault cores: an example from the Median Tectonic Line, Japan. — *Journal of Structural Geology* 28 (2), pp. 220–235.

KIRÁLY E., KOROKNAI B. 2004: The magmatic and metamorphic evolution of the north-eastern part of the Mórágy Block (A Mórágyi-rög ÉK-i részének magmás és metamorf fejlődéstörténete). — *A Magyar Állami Földtani Intézet Évi Jelentése 2003,* pp. 299–318.

KLÖTZLI, U. S., BUDA GY., SKIOLD, T. 2004: Zircon typology, geochronology and whole rock Sr-Nd isotope systematics of the Mecsek Mountain granitoids in the Tisia Terrane (Hungary). — *Mineralogy and Petrology* 81 (1–2), pp. 113–134.

KÓKAI A. 1997: Geological evaluation of the Üveghuta–1 borehole (Az Üveghuta–1 fúrás földtani értékelése) — *A Magyar Állami Földtani Intézet Évi Jelentése 1996/II,* pp. 59–75.

KOROKNAI B. 2003: Az irányított minták mikrotektonikai vizsgálata és összefoglaló értékelése (in Hungarian, translated title: Microtectonic study of the oriented samples and their summarising analysis [Üveghuta]). — *Manuscript (kézirat),* Magyar Állami Földtani Intézet, Budapest, Tekt. 1004.

KOROKNAI B. 2009: A variszkuszi orogenezishez kapcsolódó szerkezetek (Structures connected to the Variscan orogenesis). — In: BALLA, GYALOG (2009), pp. 141–149 (pp. 131–139).

KOROKNAI, B., GULÁCSI, Z. 2006: Mecsekjánosi Bazalt Formáció, alsó-kréta (in Hungarian, translated title: Mecsekjános Basalt Formation, Lower Cretaceous). — In: GYALOG et al. (2006), Chapter 4.3. (fejezet), pp. 107–118.

KOVÁCS-PÁLFFY, P., FÖLDVÁRI, M. 2004: Hydrothermal minerals and phenomena in the Mórágy Granite Formation (Hidrotermális képződmények és jelenségek a Mórágyi Gránit Formációban). — *A Magyar Állami Földtani Intézet Évi Jelentése 2003,* pp. 319–331.

LELKES-FELVÁRI, GY., FRANK, W., SCHUSTER, R. 2003: Geochronological constraints of the Variscan, Permian-Triassic and Eo-Alpine (Cretaceous) evolution of the Great Hungarian Plane basement. — *Geologica Carpathica* 54 (5), pp. 299–315.

LIN, A. 2001: S–C fabrics developed in cataclastic rocks from the Nojima fault zone, Japan and their implications for tectonic history. — *Journal of Structural Geology* 23 (6–7), pp. 1167–1178.

LONKER, S. W., FITZ GERALD J. D. 1990: Formation of coexisting 1M polytypes and 2M polytypes in illite from an active hydrothermal system. — *American Mineralogist* 75 (11–12), pp. 1282–1289.

MAROS GY. 2006: A Mórágyi Gránit szerkezeti fejlődése az ImaGeo magszkennerrel történt fúrásértékelések alapján. PhD doktori értekezés, Miskolci Egyetem (in Hungarian, translated title: Structural evolution of the Mórágy granite, based on the ImaGeo corescanner evaluations. PhD Thesis). — *Manuscript (kézirat),* Magyar Állami Földtani Intézet, Tekt. 1348.

MAROS GY., KOROKNAI B. 2009: Töréses szerkezetek (Brittle structures). — In: BALLA, GYALOG (2009), pp. 141–149 (pp. 139–145).

MAROS, GY., PALOTÁS, K. 2000a: Evaluation of planar features in Boreholes Üveghuta Üh–22 and Üh–23 with CoreDump software (Az üveghutai Üh–22 és Üh–23 fúrásban észlelt síkszerű jelenségek értékelése CoreDump szoftverrel). — *A Magyar Állami Földtani Intézet Évi jelentése 1999-ről,* pp. 315–340.

MAROS, GY., PALOTÁS, K. 2000b: Evaluation of the relative time series of events observed in Boreholes Üh–22 and Üh–23 near Üveghuta with CoreTime software (Az üveghutai Üh–22 és Üh–23 fúrásban észlelt események idősorrendjének értékelése CoreTime szoftverrel). — *A Magyar Állami Földtani Intézet Évi Jelentése 1999-ről,* pp. 341–352.

MAROS GY., BALLA Z., DUDKO A., FODOR L., FÓRIÁN-SZABÓ M., KOROKNAI B., LANTOS M., PALOTÁS K. 2003: Tektonikai zárójelentés (in Hungarian, translated title: Final tectonic report). — *Manuscript (kézirat),* Magyar Állami Földtani Intézet, Budapest, Tekt. 1046; Bátatom Kft., Budapest, BA–03–118.

MAROS GY., KOROKNAI B., PALOTÁS K., DUDKO A., BALOGH K., PÉCSKAY Z. 2009: Törészónák a Mórágyi gránitban: új szerkezeti és K/Ar adatok (in Hungarian, translated title: Brittle shear zones

in the Mórágy Granite, new structural and K/Ar data). — In: M. Tóth T. (szerk.): *Magmás és metamorf képződmények a Tiszai egységben*. Geolitera, Szeged, pp. 43–62.

Maros, Gy., Koroknai, B., Palotás, K., Fodor, L., Dudko, A., Fórián-Szabó, M., Zilahi-Sebess, L., Bán-Győry, E. 2004: Tectonic analysis and structural evolution of the north-eastern Mórágy Block (A Mórágyi-rög ÉK-i részének tektonikai elemzése és szerkezetalakulása). — *A Magyar Állami Földtani Intézet Évi Jelentése 2003,* pp. 371–394.

Maros Gy., Palotás K., Dudko A., Kovács-Pálffy P. 1999: Az Üveghuta Üh–22 és Üh–23 fúrás tektonikai vizsgálata (in Hungarian, translated title: Tectonic log of Boreholes Üveghuta–22 and 23). — *Manuscript (kézirat),* Magyar Állami Földtani Intézet, Budapest, Tekt. 644.

Márton, E., Márton, P. 1999: Tectonic aspects of a palaeomagnetic study on the Neogene of the Mecsek Mountains. — *Geophysical Transactions* 42 (3–4), pp. 159–180.

Mauritz B., Csajághy, G. 1952: Alkáli telérkőzetek Mórágy környékéről (in Hungarian, translated title: Alkali dykes in the surroundings of Mórágy). — *Földtani Közlöny* 82 (4–6), pp. 137–142.

Molnos I., Deák F., Jakab A., Somodi G., Szamos I., Vásárhelyi B. (Mecsekérc Zrt.), Gyalog L., Gulácsi Z., Maros Gy., Musitz B., Király E., Oláh I., Szebényi G. (MÁFI) 2007: Jelentés a Bátaapátiban mélyített Nyugati-lejtősakna 600,00–1309,50 és Keleti-lejtősakna 599,40–1254,10 m-es szakaszán elvégzett földtani-tektonikai, geotechnikai és vízföldtani dokumentálási munkákról (in Hungarian, translated title: Report on geological-tectonic, geotechnical and hydrogeological documentation work performed along the 600.00–1309.50 m stretch of the Western Incline and the 599.40–1254.10 m stretch of the Eastern Incline). — *Manuscript (kézirat),* Magyar Állami Földtani Intézet, Budapest, Tekt. 1381.

Molnos I., Deák F., Jakab A., Somodi G., Vásárhelyi B. (Mecsekérc Zrt.), Balla Z., Gyalog L., Gulácsi Z., Maros Gy., Palotás K., Rálisch E., Szebényi G. (MÁFI) 2006: Jelentés a Bátaapátiban mélyített lejtősaknák 0–600 fm-es szakaszán elvégzett földtani-tektonikai, geotechnikai és vízföldtani dokumentálási munkákról (in Hungarian, translated title: Report on geological-tectonic, geotechnical and hydrogeological documentation work performed along the 0-600 m stretch of inclines in Bátaapáti). — *Manuscript (kézirat),* Magyar Állami Földtani Intézet, Budapest, Tekt. 1332; Mecsekérc Zrt., Pécs, RHK–K–075/06.

Molnos I., Jakab A., Somodi G., Szamos I., Vásárhelyi B. (Mecsekérc), Gyalog L., Borsody J., Füri J., Gulácsi Z., Maros Gy., Musitz B. (MÁFI) 2008: Jelentés a Bátaapátiban mélyített Nyugati-lejtősakna 1309,50–1772,50 és Keleti-lejtősakna 1254,10–1723,50 m-es szakaszán elvégzett földtani-tektonikai, geotechnikai és vízföldtani dokumentálási munkákról (in Hungarian, translated title: Report on geological-tectonic, geotechnical and hydrogeological documentation work performed along the 1309.50–1772.50 m stretch of the Western Incline and the 1254.10–1723.50 m stretch of the Eastern Incline). — *Manuscript (kézirat),* Magyar Állami Földtani Intézet, Budapest, Tekt. 1381.

Monzawa, N., Otsuki, K. 2003: Comminution and fluidization of granular fault materials: implications for fault slip behavior — *Tectonophysics* 367 (1–2), pp. 127–143.

Nédli Zs., Szabó Cs. 2007: Az üveghutai repedéskitöltésekben megjelenő különböző ásványfázisok lehetséges geokémiai rokonságának vizsgálata. Vulkanitminták magmás rokonságának vizsgálata (In Hungarian, translated title: Study of possible geochemical relationships between various minerals of the fissure fillings at Üveghuta. Study of magmatic relationships between samples of volcanic rocks). — *Manuscript (kézirat),* Magyar Állami Földtani Intézet, Budapest, Tekt. 1375.

Némedi Varga Z. 1983: A Mecsek hegység szerkezetalakulása az alpi hegységképződési ciklusban (in Hungarian with English abstract: Structural history of the Mecsek mountains in the Alpine orogenic cycle). — *A Magyar Állami Földtani Intézet Évi Jelentése 1981-ről,* pp. 467–484.

Pană, D., Balintoni, I., Heaman, L. 2000: Precise U-Pb zircon dating of the syenite phase from the Ditrau alkaline igneous complex. — *Studia Universitatis Babeş–Bolyai, Geologia* XLV (1), pp. 79–89.

Passchier, C. W., Trouw, R. A. J. 1996: *Microtectonics.* — Springer-Verlag, Berlin, Heidelberg, New York, Barcelona, Budapest, Hong Kong, London, Milan, Paris, Singapore, Tokyo, 289 p.

Peacor, D. R., Bauluz, B., Dong, H.L., Tillick, D., Yan, Y. H. 2002: Transmission and analytical electron microscopy evidence for high Mg contents of 1M illite: Absence of 1M polytypism in normal prograde diagenetic sequences of pelitic rocks. — *Clays and Clay minerals* 50 (6), pp. 757–765.

Ramsay, J. G., Huber, M. I. 1987: *The techniques of modern structural geology. Volume II. Folds and fractures.* — Academic Press, London, 700 p.

Stewart, M., Holdsworth, R. E., Strachan, R. A. 2000: Deformation processes and weakening mechanisms within the frictional-viscous transition zone of major crustal-scale faults: insights from the Great Glen Fault Zone, Scotland. — *Journal of Structural Geology* 22 (5), pp. 543–560.

Strutinski, C., Pu, T., Stan, R. 2006: The metamorphic basement of Romanian Carpathians: a discussion of K–Ar and $^{40}Ar/^{39}Ar$ ages. — *Studia Universitatis Babeş–Bolyai, Geologia* LI (1–2), pp. 15–21.

Szongoth G., Zilahi-Sebess L., Galsa A., Bánné Győri E., Lendvay P., Bartha Z. 2003: Mélyfúrás-geofizikai adatok integrált értelmezése (az 1996–2003-ban végzett összes mérés alapján) (in Hungarian, translated title: Integrated interpretation of well-logging data (on the basis of all measurements between 1996 and 2003) [Üveghuta]). — *Manuscript (kézirat),* Magyar Állami Földtani Intézet, Budapest, Tekt. 1059; Bátatom Kft., Budapest, BA–03–62.

Tari, G. 1992: Late Neogene transpression in the Northern Imbricates zone, Mecsek Mts. Hungary. — *Annales Universitatis Scientiarum Budapestiensis de Rolando Eötvös nominatae, Sectio Geologica,* 29, pp. 165–187.

Vrolijk, P., van der Pluijm, B.A. 1999: Clay gouge. — *Journal of Structural Geology* 21 (8–9), pp. 1039–1048.

Wein Gy. 1961: A szerkezetalakulás mozzanatai és jellegei a Keleti-Mecsekben (Phasen und Beschaffenheit der tektonischen Ausbildung im östlichen Mecsek-Gebirge). — *A Magyar Állami Földtani Intézet Évkönyve* 49 (3), pp. 759–768 (pp. 945–956).

Wein Gy. 1965: Az Északi Pikkely a Mecsek hegységben (in Hungarian, translated title: The Northern Imbricates in the Mecsek Mts.). — *Bányászati és Kohászati Lapok, Bányászat* 98 (6), pp. 402–411.

Wein Gy. 1967: Délkelet-Dunántúl hegységszerkezeti egységeinek összefüggései az óalpi ciklusban (in Hungarian with German abstract: Zusammenhänge der tektonischen Einheiten Südost-

Transdanubiens im altalpidischen Zyklus). — *Földtani Közlöny* 97 (3), pp. 286–293.

WIBBERLEY, C. A. J., SHIMAMOTO, T. 2003: Internal structure and permeability of major strike-slip fault zones: the Median Tectonic Line in Mie Prefecture, Southwest Japan. — *Journal of Structural Geology* 25 (1), pp. 59–78.

ZILAHI-SEBESS L. 2005: Mélyfúrás-geofizikai mérések értelmezése a Mórágyi rög területén. PhD doktori értekezés (in Hungarian, translated title: Interpretation of well-logging measurements in the area of the Mórágy Block. PhD Thesis). — *Manuscript (kézirat),* Eötvös Loránd Tudományegyetem, Természettudományi Kar, Budapest.

ZILAHI-SEBESS, L., MÉSZÁROS, F., SZONGOTH, G. 2000: Characterisation of fracture zones in granite, based on well-logging data at the Üveghuta Site (A gránit töréses öveinek jellemzése mélyfúrás-geofizikai adatok alapján az üveghutai telephelyen). — *A Magyar Állami Földtani Intézet Évi Jelentése 1999-ről,* pp. 253–272.